



COMOTI
ROMANIAN RESEARCH &
DEVELOPMENT INSTITUTE FOR
GAS TURBINES

TURBO

Scientific Journal

vol. X (2023), no. 1

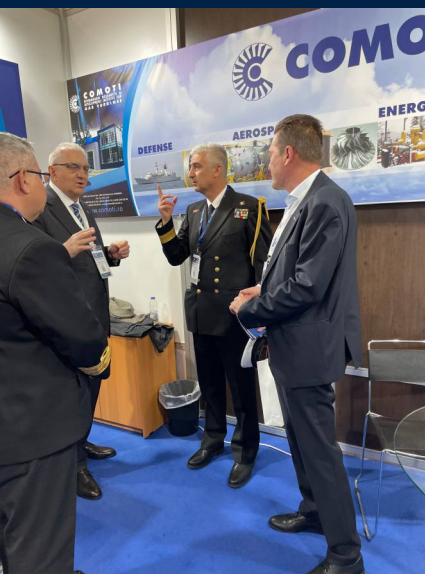


9-11 MAY 2023
Defence Exhibition Athens
INTERNATIONAL DEFENCE & SECURITY EXHIBITION

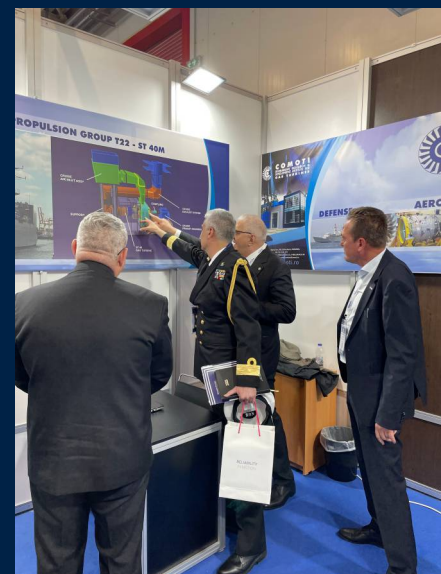
www.defea.gr



COMOTI - Romanian Research & Development Institute for Gas Turbines attended DEFEA - Defence Exhibition Athens between 9-11 May 2023.



- We were happy to be here and meet so many interesting and important professionals from the Defense Industry.
- Our new naval propulsion system, based on a Canadian-made ST40M aero derivative turbo engine, attracted the attention of many specialists.
- The system was designed, developed, tested and successfully installed on the Romanian frigates.
- We had important meetings with officials from the Hellenic Navy and Romanian Navy where we discussed about the possibility of future collaborations.



PRESIDENT:

Dr. Eng. Valentin SILIVESTRU

VICE-PRESIDENT:

Dr. Eng. Romulus PETCU
Dr. Eng. Cristian CARLANESCU

TECHNICAL SECRETARY:

Dr. Eng. Jeni VILAG

MEMBERS:

Prof. Dr. Virgil STANCIU
Prof. Dr. Corneliu BERBENTE
Prof. Dr. Dan ROBESCU
Prof. Dr. Sterian DANAILA
Conf. Dr. Ing. Daniel-Eugeniu CRUNTEANU
Conf. Dr. Ing. Grigore CICAN
Mat. Dr. Ing. Catalin NAE
Dr. Eng. Gheorghe MATAACHE
Dr. Eng. Ene BARBU
Dr. Eng. Gheorghe FETEA
Dr. Eng. Valeriu VILAG
Dr. Eng. Ionuț PORUMBEL
Dr. Eng. Valeriu DRAGAN
Dr. Eng. Lucia Raluca MAIER
Dr. Eng. Andreea MANGRA
Dr. Eng. Sorin GABROVEANU

EDITOR IN CHIEF:

Prof. Dr. Lacramioara ROBESCU

EDITORS:

Dr. Eng. Mihaela Raluca CONDRUZ
Ec. Elena BANEA

ADMINISTRATIVE SECRETARY:

Eng. Mihaela GRIGORESCU

TRANSLATION CHECKING:

Dr. Eng. Ionut PORUMBEL
Oana HRITCU

GRAPHICS:

Victor BESLEAGA

More information:
[http://www.comoti.ro/ro/
jurnalul_stiintific_turbo.htm](http://www.comoti.ro/ro/jurnalul_stiintific_turbo.htm)
jeni.vilag@comoti.ro

ISSN: 2559-608X
ISSN-L: 1454-2897

Scientific Journal TURBO is included in:

-ICI World of Journals:

ICV 2021: 83,53

<https://journals.indexcopernicus.com/search/details?id=48512>

**-Directory of Open Access Scholarly Resources
(ROAD)**

<https://portal.issn.org/resource/ISSN/2559-608X#>

-Directory of Research Journals Indexing (DRJI):

<http://olddrji.lbp.world/JournalProfile.aspx?jid=2559-608X>

- ♦ *Editorial*2

GAS TURBINE ENGINES

- ♦ *Instrumentation and data acquisition system for microjet engines - prototypes*

C.M. Tarabic, C. Olariu, G. Cican, G. Dediu, R.A. Se-careanu, C.P. Suci, A. Hank 6

MATERIALS AND TECHNOLOGIES

- ♦ *Designing the actuation system of an electric bicycle with photovoltaic panels*

M. Roman, D. Lale, R. Stoica 14

GAS DYNAMICS

- ♦ *STV for an RTJ, using a PIV commercially available post-processing software*

E.G. Prisacariu 25

SCIENTIFIC MANAGEMENT

- ♦ *Development of strategic management performance metrics for projects financial monitoring*

M.C. Arvinte 40

Editorial

Ce poate oferi arta într-un moment de criză? (1)

Pe ea însăși, într-o imagine mediată a obiectului sau subiectului.

Suferința și furia lumii ajung în artă și se întorc la privitor într-o fragilitate rezistentă care naște un moment de contemplare ce ne poate conduce la înțelegerea propriei finitudini, ca pretext în același timp pentru înțelegerea contextului traumatic. Izolarea, moartea și singurătatea sunt lucruri de care niciunul dintre noi nu este scutit.

Dintre numeroasele paradoxuri ale artei, poate cel mai frapant este acela de combinare a comentariului social acut cu exprimarea și realizarea dorințelor complet imposibile, în intenția de a crea o lume transformată sau o societate alternativă. Orice reprezentare atrage după sine problema conținutului ei.

Prin artă se poate atinge punctul post-contemplare, prin revizuirea experiențelor personale, ca mijloc de arhivare a emoției pe căi obiective printr-un dialog permanent cu memoria, cea personală și cea istorico-socială. Pornind de la aici și acum, se conturează intuiția spațiului. Raportul dintre om și spațialitate se întemeiază pe două simțuri aflate deopotrivă în dispută și în complicitate: simțul văzului și simțul tactil.

În exegeza creștină, acest conflict al determinării existenței prin simțuri ne este înfățișat prin întâlnirea dintre Toma Necrednciosul și Iisus: doar atingându-I coasta lui Iisus, Toma va crede. Percepția vizuală curentă poate oricând să fie infirmată de o percepție vizuală viitoare, dar atingerea oferă certitudinea incontestabilului.

Spațiul publicului, al consumatorului de artă, este un spațiu al distanței, căruia îi revine ca mod de înțelegere doar văzul ca simț al distanței prin excelență, în același timp perceperea celuilalt păstrându-se în sfera vizualului.

Pentru Edmund Husserl* punctul de plecare în constituirea lumii rămâne trupul, dar trupul înzestrat cu simț tactil, căci un trup care are doar văz este lipsit de înțelegerea și cuprinderea spațială. El subliniază clar că punctul de orientare în lume, în înțelegerea și cuprinderea spațială rămâne propriului corp, iar primordial rămâne simțul tactil.

Estetica - știința neutilizării sau relația omului contemplativ cu latura creatoare a realității, studiază legile și categoriile artei și este considerată drept forma cea mai înaltă de creare și de receptare a frumosului, prin ansamblu de probleme privitoare la esența artei, la raporturile ei cu realitatea, la metoda creației artistice, la criteriile și genurile artei.

* Filozof și matematician, considerat fondatorul fenomenologiei, considera că experiența este sursa cunoașterii, 8 aprilie 1859, Prostějov, Moravia, Imperiul Austriac – 26 aprilie 1938, Freiburg, Germania

Editorial

Ce poate oferi arta într-un moment de criză? (2)

Termenul de estetică este folosit în literatura științifică contemporană și în viața de zi cu zi și într-un sens diferit, pentru a desemna componenta estetică a culturii și a componentelor sale estetice. În acest sens, este vorba despre estetica de desfășurare a unei activități, căci experiența estetică este inerentă evoluției omului din cele mai vechi timpuri, când a descoperit expresia sa inițială prin practică, în încercări de a crea acele fenomene care astăzi fac parte din sfera artei și totodată printr-un efort de a-și înfrumuseța viața, într-o zbatere eliberatoare, prin realizarea de podoabe ori obiecte utilitare sau aparținând ritualurilor religioase, militare ori activităților sportive.

Potrivit lui Friederich Schiller**, experiența estetică, în special arta, ajută o persoană să-și găsească libertatea și fericirea pe care omul le-a pierdut odată cu dezvoltarea civilizației.

Civilizațiile, în dezvoltarea lor, au cunoscut crize. Criza se conturează cel mai adesea atunci când se dezintegrează sistemul de valori stabilit de secole. Criza apare și atunci când un frate se duce peste fratele său, fiu al tatălui său, atunci când copiii sunt uitați de către părinții lor iar cenușa strămoșilor este împrăștiată de vânturile războaielor.

La cine se află resortul eliberării dintr-o criză ?

Eliberatorul prin excelență este ființa care s-a eliberat prima!

Ec. Elena Banea

***Scieri estetice*, traducere și note de Ciorogaru, Gheorghe, Ed. Univers, București, 1981

Editorial

What can art offer during a crisis period? (1)

It's the art itself, as a transposed image of the object or subject.

All the world suffering and fury are assimilated into art and get back to the onlooker with a resilient fragility that triggers a moment of contemplation that may lead us to the understanding of our own limitations and which may also serve as a pretext for the understanding of a traumatic background. Isolation, death and loneliness are such situations that none of us is exempted from.

Of various paradoxes of art, perhaps the most shocking of all is the mixture of keen social comment with expression and fulfillment of utterly impossible aspirations, in an attempt to create a transposed world or an alternative social environment. Any representation entails the very problematic nature of its content.

Art helps us reach a post-contemplation moment, while re-examining personal experiences, as a means of recording emotion in objective ways, through a permanent dialogue with both the individual and socio-historical memory. It is from this very point that the intuitive perception of space is starting to out-line itself. The connection between man and space is based on two senses, which are in dispute and complicity all at once: the sense of sight and the tactile sense.

According to the Christian exegesis, this conflict in determining the existence through senses is artistically represented for us in the meeting of Faithless Thomas and Jesus: the mere touch of Jesus' rib will simply turn Thomas into a believer. The current visual perception may be anytime denied by a future visual perception, but the touch offers the certainty of the indisputable.

The environment of the audience, that is, of the art consumer's, is a space of perspective, which can be understood only by using sight as a main means of perspective appreciation, while, at the same time, the perception of another individual is basically placed within the visual area.

For Edmund Husserl*, the starting point in building up the world is the body itself, but the one endowed with a tactile sense, since a body endowed with sight only is lacking both spatial understanding and perspective. He clearly underlines the fact that the orientation point in the world around, which is used for spatial understanding and perspective, is an attribute of our own body, with the tactile sense having a primordial role.

Aesthetics - the science of inaction or the relationship of the contemplating man with the creative side of reality, studies the art laws and categories and it is considered the most elevated form of creation and reception of the beauty, due to the overall issues related to the essence of art, to its connections with reality, the method of artistic creation or to the criteria and genres of art.

* Philosopher and mathematician, considered to be the founder of phenomenology, who considers that experience is the source of knowledge, 8 April 1859, Prostějov, Moravia, the Austrian Empire– 26 April 1938, Freiburg, Germany

Editorial

What can art offer during a crisis period? (2)

The very term of aesthetics is being used in contemporary scientific literature, as well as in every day life, and yet in a distinct sense in order to define the aesthetic component of culture and of its aesthetic subparts. In this sense, we refer to the aesthetics in the development of an activity, as the aesthetic experience is inherent to human evolution since ancient times, when man discovered his/her initial ways of expression through practice, in his/her attempt to determine those phenomena that are included today within the art universe, and also through an effort to make his life more attractive, through a liberating strife, by creating ornaments, utilitarian objects or things serving him in religious and military rituals or sport activities.

According to Friederich Schiller**, aesthetic experience, arts in particular, helps an individual to discover the liberty and happiness that man has lost during the development of civilization.

Along their developing process, civilizations have encountered various crises. Most often, a crisis occurs when the pre existent secular system of values disintegrates itself. A crisis may also be represented by a brother's attack over his own brother, that is, his father's own son or when children are being forgotten by their parents, and the ancestors' ashes is vanished by the gales of wars.

Who does posses the resort of liberation in a moment of crisis?

Above all, the liberator is that very individual who has managed to release him/herself first!

Ec. Elena Banea

**Aethetic Writings, translation and notes by Ciorogaru, Gheorghe, Universe Printing House, Bucharest, 1981

INSTRUMENTATION AND DATA ACQUISITION SYSTEM FOR MICROJET ENGINES – PROTOTYPES

Cornel Mihai TĂRĂBÎC^{1,2}, Cristian OLARIU¹, Grigore CICAN², Gabriel DEDIU¹, Rareş Andrei SECĂREANU¹, Cosmin Petru SUCIU¹, Alexandru HANK¹

Received: 25.11.2022

Accepted: 29.01.2023

Published: 14.07.2023

Copyright: The article is an Open Access article and it is distributed under the terms and conditions Creative Commons Attribution (CC BY) license (<https://creativecommons.org/licenses/by/4.0/>).



ABSTRACT: This paper presents a methodology of testing microjet engine that consists of instrumentation, data acquisition & control system and graphical user interface. The presented methodology applies only for general studies that are performed on prototype engines. In order to provide all the necessary facilities for the experimental campaign, a series of elements are required (such as, a data acquisition & control system, instrumentation for the engine & test bench and the specific software program for testing in automated mode, using LabVIEW). The main data acquisition and control system is a cDAQ 9189 and 8 modules from National Instruments that can acquire all the necessary data and control the auxiliary system and the engine. The instrumentation consists of different types of sensors, transducers and control elements that are synchronized in cDAQ. The experimental campaign was planned based on the specific testing procedure that considers the startup regime, the working regime and the stopping regime. The results were acquired using the specified instrumentation and the data acquisition system. The most important parameters are presented for the starting and idle regimes, in order to validate the methodology.

KEYWORDS: microjet engine, instrumentation, acquisition, LabVIEW, experimental campaign

NOMENCLATURE

cDAQ	Compact data acquisition
DACS	Data acquisition and control system
UAV	Unmanned aerial vehicle
APU	Auxiliary power unit
NI	National Instruments
VI	Virtual Instrument
N_{ref}	Reference speed
N_{cor}	Corrected speed
N	Speed

¹ Romanian Research and Development Institute for Gas Turbines COMOTI

² University Politehnica of Bucharest, Faculty of Aerospace Engineering

$T4$	Turbine outlet temperature
$T3$	Turbine inlet temperature
QcT	Total fuel flow
QcM	Combustion chamber fuel flow
QcU	Lubrication flow
Pcb	Fuel pressure
$URTP$	Fuel pump control tension
IPC	Fuel pump current
F	Thrust
$Ma - c$	Corrected air flow
$N\%$	Actual speed reported to the maximum speed
dQc	The difference between the total flow and the sum of the combustion chamber and lubrication flow
$Pair$	Pneumatic starter air pressure
$Pgas$	Gas pressure
VIB	Engine vibration
$T0$	Test cell temperature
$P0$	Test cell pressure
dPv	Intake bellmouth differential pressure
$T1$	Intake bellmouth total temperature
$P1$	Intake bellmouth total pressure
$P2T$	Compressor outlet total pressure

1. INTRODUCTION

Generally, microjet engines are gas turbines at lower scale, that produces thrust force and also has similar functional proprieties but with a few particularities. For example, compact dimension, high operating speed, easier operability, lower NOx emission, lower maintenance costs [1]. To conduct different studies using commercial or prototypes engines, it can be more convenient to perform the experiments on a specific test bench, hence the costs are lower than the gas turbine engines. Some studies were made regarding the feasibility on this category and even on ultra and nano gas turbine [2]. The micro gas turbines can develop an output in range of **15 kW ÷ 300 kW** and even exceed the power of **1000 kW** using special technologies [3].

In present, the microjet engines are used for applications, such as, UAV [4], as auxiliary power unit APU [5] or as low power plants, for electrical generators [6]. The first appearances of microjet engines happened around the years 1950-1970 in the field of automotive fields [7] although they were developed for other purposes, such as generators of electrical energy in stationary rocket launchers, engines for buses or other methods of transport [8].

One of the most important phases of developing an microjet engine, consists in the experimental campaign that validates all the necessary features and establishes the working regimes and performances. Microjet engines are suitable for these types of applications, mentioned earlier, due to their high power-to-weight ratio, where the performances of the main components dictate overall engine performance [9].

The experimental campaign needs to satisfy a series of requirements, especially when is monitored at different ambient conditions at the test bench, due to the modifications that are present in the atmosphere and also, while using the transient process, acceleration, in both ways, such as, normal acceleration and sudden acceleration [10]. Developing a testing procedure for a prototype engine is different than using a manufactured engine, since it's not based on an engine manual and needs to be determined in other ways [11].

To carry out the experimental campaign based on the defined facilities, a data acquisition and control system was proposed. Furthermore, the instrumentation is extended in order to obtain sufficient data to determine the characteristics and performances for the engine.

2. DACS AND INSTRUMENTATION FOR ENGINE/ TEST BENCH

In order to provide all the necessary facilities, the test bench is divided in three parts. The first part contains the mechanical assemblies and subassemblies to install the engine and the auxiliary system required. The second part consists of the data acquisition system that manages the information taken from the engine, the auxiliary systems and the test cell and sent it to the main computer in real time that stores it to create the post-processing element. The third part is formed by the instrumentation for the engine, for test cell and for auxiliary systems in order to monitor all the parameters and have control over the systems.

To monitor all the parameters, a series of different types of sensors and transducers were used. Due to the fact that the system is designed to have a prototype engine for testing, the instrumentation is extended for different sections of the engine.

Based on the general scheme provided in Fig. 1, the system was built in order to use the compact DAQ chassis 9189 from National Instruments [12] due to the specifications in terms of precision, high acquisition rate of the modules/ chassis. The LabVIEW software was used due to its main characteristics that covers from the channel settings to the storing settings, and also can create a particularly automated command and control algorithm. The cDAQ 9189 has 8 slots and the configuration is the following: for thermocouples NI 9213 [13], for resistance temperature detector NI 9216 [14], two for voltage input NI 9205 [15], for vibration and sound NI 9232 [16], for voltage output NI 9264 [17], for digital output NI 9474 [18].

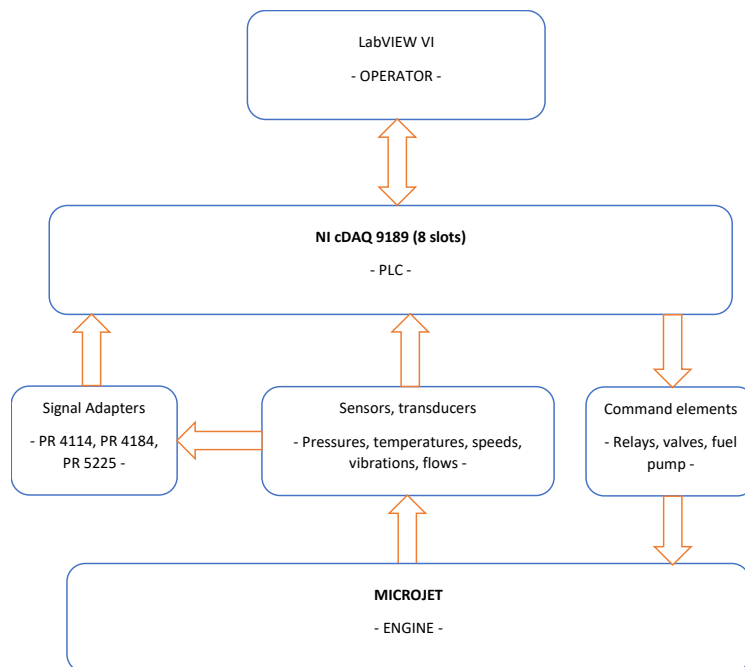


Fig. 1 - General schematic of the data acquisition system and instrumentation

The pressure transducers, the flow meters and the speed sensor were connected with signal adapters in order to convert from current (for pressure and flow meters) or frequency (for speed sensor) to voltage. These voltage signals are connected to the NI 9205 module. The thermocouples and resistance temperature detector (RTD) were connected directly to their specific module, the NI 9213 and NI 9216. The measured tension from different equipment's, was directly connected to the first and second NI 9205. In order to control the engine, a fuel pump and a series of valves were used as a part of the auxiliary systems.

The test cell is equipped with a pressure and a temperature sensor to monitor the ambient parameters. It also has a video system, in order to record any unforeseen situation.

The auxiliary systems are composed of:

- The fuel system that is designed for fuel supply and lubrication. Also, the instrumentation on the fuel line is: three supply valves, one located at the exit of the fuel tank, one located at the entrance of the engine for fuel supply and the third one, for the lubrication, a pressure sensor before the flow meters, three flow meters, one for the fuel supply of the engine, one for fuel lubrication and one for the total flow, a temperature sensor and a fuel pump. Also, the fuel lines have a bypass system, in order to decrease the fuel pressure;

- The air system that is designed for starting the engine. Also, the instrumentation on the air line is: a supply valve and a pressure sensor at the engine inlet;
- The gas system that is designed for fuel supply at the start of the engine. Also, the instrumentation of the gas line is: two supply valves, one located near the gas tank and one located at the entrance of the engine, a pressure and temperature sensor at the engine inlet.

The engine instrumentation is divided based on the section of the engine:

- On the section of the inlet, a differential pressure was used in order to determine the air flow, a static pressure and a total temperature;
- On the section of the compressor, a total pressure, a static pressure and a total temperature was used;
- On the section of the combustion chamber, a total pressure, a static pressure, three total temperatures and determined for the average temperature;
- On the section of the turbine, a total pressure, a static pressure and three total temperature and determined for the average temperature.

Based on the instrumentation and the control system, a program was created using LabVIEW DAQmx programming environment. The VI presented in Fig 2. has the capability of monitoring the parameters in real time using Front Panel function, to use different types of controlling methods in automated capabilities and to record the input and output parameters at a designated acquisition rate. Every panel is envisioned with a specific usefulness, one for the starting phase (named "Starting regime"), one that contains every parameter recorded and calculated (named "Parameters") and one for the working regime (named "Working Regime"). When the test begins, all the parameters are recorded in real time with the defined acquisition rate, configured in the Block Diagram.

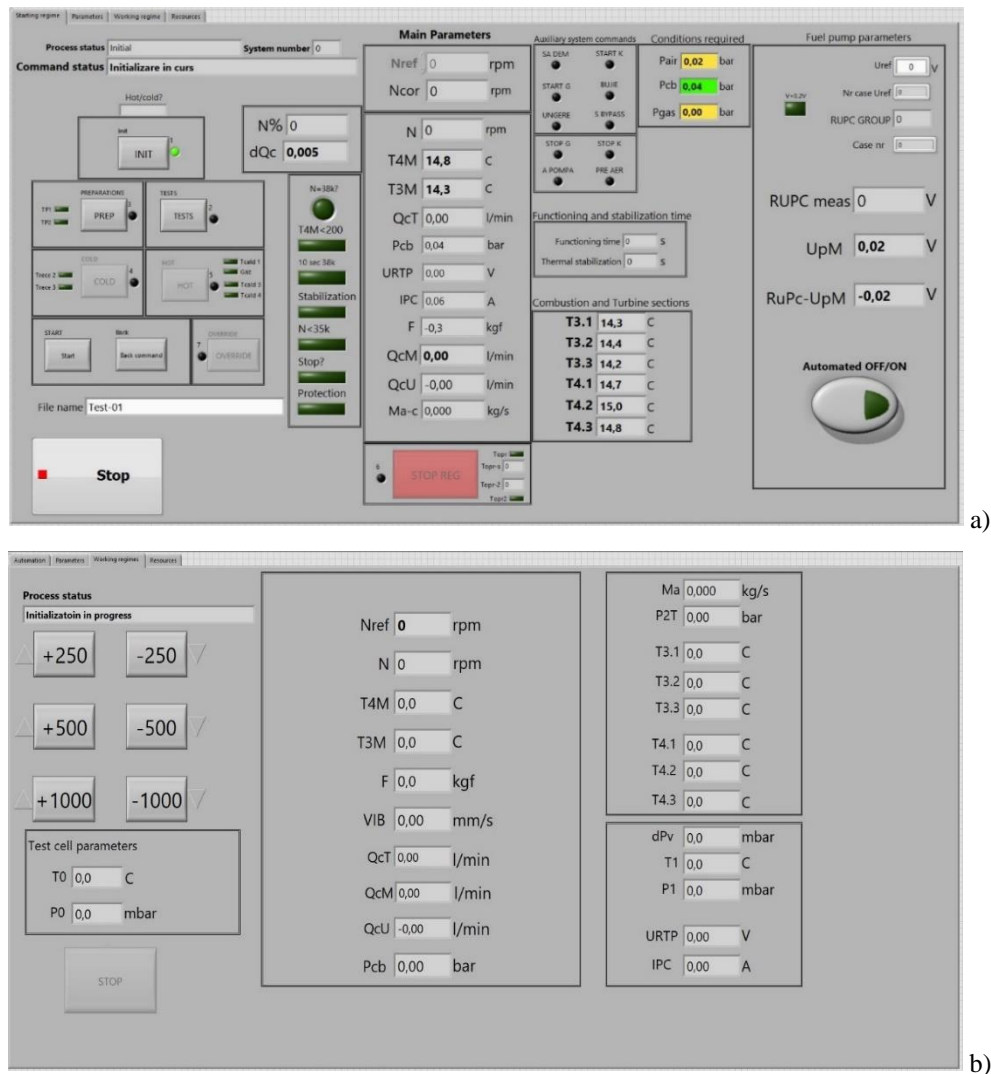


Fig. 2 a) The operator interface for starting regime; b) The operator interface for Working regime

The starting phase consist of using some parameters as inputs and setting different commands for the digital output and the fuel pump in a successive algorithm. Before it runs on the cold start or the hot start, a set of conditions are need to be met, especially regarding the fuel, gas and air parameters (the process is named the “Initialization in progress”). If the conditions are met, the starting is visible on the operator front panel and can the process can begin.

After the starting procedure and thermal stabilization, the “Working regime” interface is ready to control the engine from idle to the maximum using N_{ref} . The experimental error of the instrumentation is generated by the sum of: the sensor/transducer error plus the signal adapter error, if it is used, plus the module of the main chassis error.

3. EXPERIMENTAL CAMPAIGN

The experimental procedure is based on a successive algorithm that is using the input parameters as conditions to be met and set the commands and controls for the fuel, gas and air lines and controls the fuel pump in accordance with the imposed conditions. The starting process is automated and it begins with the air supply on the compressor, in order to spin the rotor, then begins the burning phase with butane gas and after a certain speed, the kerosene starts to be injected in the combustion chamber in the same time as the butane gas. After a certain speed, the butane gas and air supply are stopped, working only on kerosene and can reach the idle regime. The prototype installed on the test bench is presented in Fig 3. with the instrumentation and the auxiliary system.

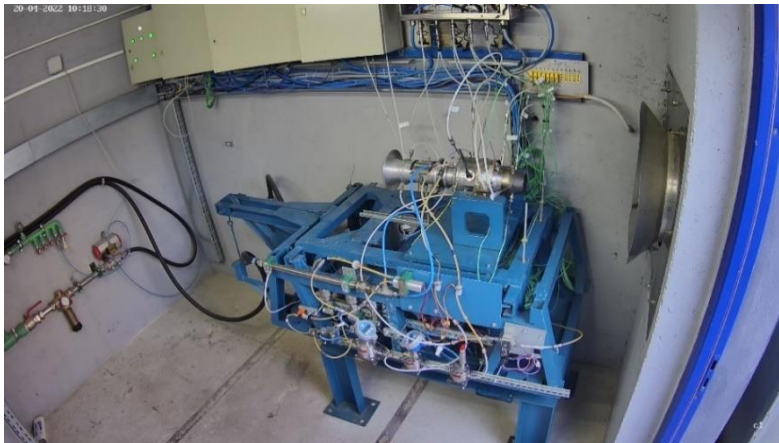


Fig. 3 The prototype installed on the test bench

One of the most important parts of experimenting with a microjet engine is the starting regime, hence it only contains transient process. In this regime, the parameters vary significantly in a relative short time and must be carefully monitored in order not to exceed the defined limits. If the limit is exceeded, a set of algorithms must be established to stop the engine operation in a short time without damaging the components. This algorithm must be in pair with the most important parameters, such as speed, turbine temperature, vibration and also, with the control of the fuel pump. Before the experimental campaign was carried out, a set of verifications and pre-tests were conducted in order to verify the functionality of the instrumentation and software. Also, the software was simulated in order to check the data flow and the order sequence for the control algorithm that was used in the starting and working phases.

The engine was tested only in the starting and idle regimes, in order to validate the automated algorithm and the testing program. The parameters were acquired at specified acquisition rate of **10 Hz** and recorded with the same rate. The specified acquisition rate was set in order to use the high measuring precision [19].

4. RESULTS

Based on the experimental campaign, a series of results are presented in Fig. 4. After the completion of the experiments, the data was stored as excel files in order to perform the post-processing of the data.

To validate the methodology, the raw data for the speed and other important parameters are presented below for starting regime and idle regime. The speed has a sudden slope at the starting, in order to reach idle regime around half of minute. The main purpose of this is to exceed all the transient process that occurs. After this, the engine is stabilizing around $N = 40000 \text{ rpm}$.

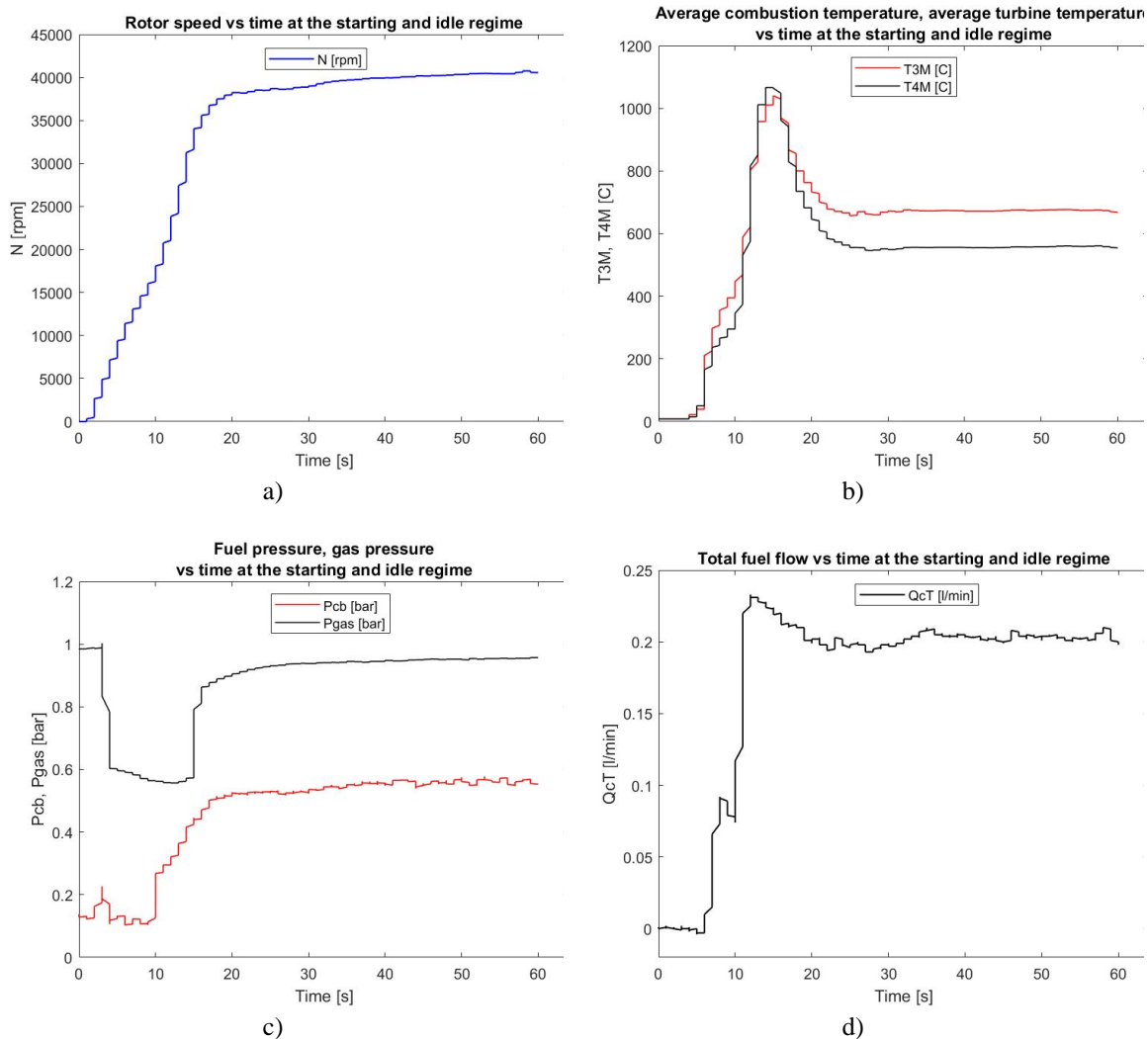


Fig. 4 a) Rotor speed vs time for the starting and idle regimes; b) Average combustion chamber and turbine temperature vs time for the starting and idle regimes; c) Fuel and gas pressure vs time for the starting and idle regimes; d) Total fuel flow vs time for the starting and idle regimes

The average combustion chamber and turbine temperature has a slower rise at the beginning due to starting with butane gas and when the kerosene is introduced in the combustion chamber, the slope has a more sudden rise. At the idle regime, the temperatures stabilize and can be considered constant.

The high gas pressure indicates the valve is closed. When the engine starts, the gas pressure decreases to a certain value and is maintained constant. There is a moment, when the fuel pressure starts to increase and the gas pressure is constant, both gas and kerosene are introduced in the combustion chamber. When the gas pressure rises back to **0.8 bar**, the gas is turned off and the engine runs only on kerosene. The total fuel flow, indicates when the kerosene is actually introduced in the combustion chamber. The variation at the idle mode it can be considered low, compared to the variations from the starting regime.

5. CONCLUSIONS AND FURTHER WORK

This article presents a study for the methodology regarding microjet engines instrumentation, data acquisition and control system and experimental campaign in order to obtain sufficient data for evaluating the performances and the functionality of a prototype engine, as well as the auxiliary systems. It describes the general schematic for a DACS system, using cDAQ 9189 with their specified modules and a specific set of instrumentation. The LabVIEW program developed was made based on a specific testing procedure in order to realize the automated algorithm for starting the engine and to control it, after the idle regime to the maximum regime. The results, were presented as raw data in order to visualize the capabilities of the system and the programming logic behind.

For future work, the LabVIEW program will include a sequence that controls the “Emergency Stop” in order to prevent the damage to the prototype engine when an unforeseen situation occurs. Furthermore, the control of the fuel pump can be improved by using PID methodology and a comparison study can be made, with the current methodology using proportional control.

ACKNOWLEDGEMENT

This work was supported by the Romanian Research and Development Institute for Gas Turbines COMOTI.

REFERENCES

- [1] T. Stevens, F. Verplaetsen, M. Baelmans „Requirements for recuperators in micro gas turbines”, Katholieke Universiteit Leuven, Dept. of Mech. Engineering, div. TME Celestijnenlaan 300A, B-3001 Leuven-Heverlee, Belgium;
- [2] Capata, Roberto & Enrico, Sciubba. (2006). Preliminary Considerations on the Thermodynamic Feasibility and Possible Design of Ultra-, Micro- and Nano-Gas Turbines. International Journal of Thermodynamics. 9. 10.5541/ijot.171;
- [3] Isaias Hernandez-Carrillo, Christopher Wood, Hao Liu, „Development of a 1000 W organic Rankine cycle micro-turbine-generator using polymeric structural materials and its performance test with compressed air”, Energy Conversion and Management, Volume 190, 2019, ISSN 0196-8904, <https://doi.org/10.1016/j.enconman.2019.03.092>;
- [4] J Dutczak, „Micro turbine engines for drones’ propulsion”, Scientific Conference on Automotive Vehicles and Combustion Engines (KONMOT 2016), IOP Conf. Series: Materials Science and Engineering 148 (2016) 012063 doi:10.1088/1757-899X/148/1/012063;
- [5] T.V. Trebunskikh, A.V. Ivanov, G.E. Dumnov, „FloEFD simulation of micro-turbine engine”, Mentor Graphics, Moscow, Russia, 2012;
- [6] Terrence W. Simon and Nan Jiang, „Micro- or Small- Gas Turbines”, Department of Mechanical Engineering Heat Transfer Laboratory University of Minnesota;
- [7] R M R A Shah*, A McGordon, M Amor-Segan, P Jennings, „Micro Gas Turbine range extender - Validation techniques for automotive applications”, University of Warwick, United Kingdom, January 2014;
- [8] Micro Gas Turbine Technology Research and Development for European Collaboration, Technology Summary, <https://etn.global/research-innovation/rd-reports/>;
- [9] Diamantis Bakalis, A. G. Stamatias, „Data analysis and performance model calibration of a small turbojet engine”, Proceedings of the Institution of Mechanical Engineers Part G Journal of Aerospace Engineering DOI: [10.1177/0954410011425126](https://doi.org/10.1177/0954410011425126);
- [10] Cican, G., Toma, A., Pușcașu, C. et al. Jet CAT P80 Thermal Analyses and Performance Assessment Using Different Fuels Types. J. Therm. Sci. 27, 389–393 (2018). <https://doi.org/10.1007/s11630-018-1026-z>;
- [11] Catana, R.M.; Cican, G.; Dediu, G. Gas Turbine Engine Starting Applied on TV2–117 Turboshift. Eng. Technol. Appl. Sci. Res. 2017, 7, 2005–2009;
- [12] National Instruments; 2022; cDAQ-9189 Specifications; <https://www.ni.com/docs/en-US/bundle/cdaq-9189-specs/page/specs.html>;
- [13] National Instruments; 2022; NI 9213 datasheet; <https://www.ni.com/docs/en-US/bundle/ni-9213-specs/page/overview.html>;

- [14] National Instruments; 2021; NI 9216 datasheet; <https://www.ni.com/docs/en-US/bundle/ni-9216-specs/page/specs.html>;
- [15] National Instruments; 2021; NI 9205 datasheet; <https://www.ni.com/docs/en-US/bundle/ni-9205-specs/page/specifications.html>;
- [16] National Instruments; 2021; NI 9232 datasheet; <https://www.ni.com/docs/en-US/bundle/ni-9232-specs/page/specs.html>;
- [17] National Instruments; 2021; NI 9264 datasheet; <https://www.ni.com/docs/en-US/bundle/ni-9264-specs/page/specs.html>;
- [18] National Instruments; 2021; NI 9474 datasheet; <https://www.ni.com/docs/en-US/bundle/ni-9474-specs/page/specifications.html>;
- [19] Catană, R.M.; Dediu, G.; Tărăbîc, C.M. Studies and Experimental Research in the Evaluation of TV2-117A Turbohaft Engine Working Regimes. *Appl. Sci.* 2022, 12, 3703. <https://doi.org/10.3390/app12073703>

Disclaimer/Publisher's Note: The statements, opinions and data contained in all publications are solely those of the individual author(s) and contributor(s) and not of COMOTI or the editor(s). COMOTI and/or the editor(s) disclaim responsibility for any injury to people or property resulting from any ideas, methods, instructions or products referred to in the content.

DESIGNING THE ACTUATION SYSTEM OF AN ELECTRIC BICYCLE WITH PHOTOVOLTAIC PANELS

Mihaela ROMAN^{1,2}, Daniel LALE^{1,2}, Remus STOICA¹

Received: 21.04.2023
Accepted: 06.06.2023
Published: 14.07.2023

Copyright: The article is an Open Access article and it is distributed under the terms and conditions Creative Commons Attribution (CC BY) license (<https://creativecommons.org/licenses/by/4.0/>).



ABSTRACT: This paper presents the designing process of an electric vehicle using power from photovoltaic energy harvesting technology. The motor, batteries and photovoltaic panels of the assembly have been chosen according to the pre-established operating parameters of the system with respect to the speed and acceleration desired for the assembly. The positioning of the photovoltaic panels is discussed, keeping in mind the comfort and efficiency of the electric bicycle, but also considering the social factor of the structure. The performance results are presented and compared to a different method of calculating the power of the motor. The study herein pursues a future application of energy harvesting through the optimization of the photovoltaic panels' performance and improving the energy conversion efficiency. The paper brings an original design through the placing of the solar panels on the fenders, not adopting the common rooftop solution.

KEYWORDS: Electric Vehicle, Energy Harvesting, Photovoltaic Panels, Solar Energy

NOMENCLATURE

PV – Photovoltaic Panels
EV – Electrical Vehicle
E-bikes – Electric Bicycles
MPPT – Maximum Power Point Tracking
NPPT – Normal Power Point Tracking
 P_{VE} – Required Power for the Electrical Vehicle
 T_{VE} – Required Torque for the Electrical Vehicle
 $C_{battery}$ – Battery Capacity
 $C_{discharge}$ – Battery Discharge
 E_{full_charge} – Battery Energy for Full Charge
 P_{solar_output} – Solar Power Output
 $P_{adjusted}$ – Solar Power Output with Losses
 t_{charge} – Estimated Charging Time

¹ Romanian Research and Development Institute for Gas Turbines COMOTI, Automation and Electrical Engineering Department.

² University Politehnica of Bucharest.

1. INTRODUCTION

One of the largest sources of air pollution in urban areas is generated by transportation. For the development of national sustainability strategies, governments have started to promote bicycles as an alternative mode of transportation to replace private cars, since the very beginning of this century [1], especially in urban areas where the terrain and the roads allow it [2]. One of the alternatives that have started gaining popularity due to its efficiency is using photovoltaic panels (PV) for multiple applications [3]. One of the applications that are still being exploited is using the capability of harvesting solar energy through the solar cells of the PV [4] and storing it into batteries, therefore being able to use this energy to power up the motor for an electrical vehicle (EV).

Electric bicycles (e-bikes) are becoming a sustainable alternative to traditional automobile transportation. An electric bike [5-7] includes all the benefits that conventional bicycles have to offer, as well as faster, more comfortable and longer trips, and less effort for the user [2]. The use of electric bicycles is a non-polluting eco-friendly means of transportation. However, recharging the batteries might be inconvenient and costly, considering the rising price of electricity. Coming in response to this issue, we propose an e-bike with solar panels [8-10] for battery recharging. There are numerous different things that affect the energy use of e-bikes. The energy requirements will vary heavily depending on the choice of route, the rider's weight, the e-bike's specifications, etc. A few of these parameters were identified in the literature review but some are dependent on actual system design [9].

In this paper, we propose and discuss a design for an EV system powered by PVs in a manner that is efficient for energy harvesting, displacing from one location to another in the urban area and has a non-intimidating and easy to use hardware structure. The components proposed for this study, as well as the most effective placement of the PV panels and the results obtained after the acquisition of data will be discussed for maximum power point tracking (MPPT), in the most optimal conditions and for a normal power point tracking (NPPT), representing the influence of multiple possible factors, such as time of the day and shading.

This is a relevant direction for new product development since PV technology can contribute to improved features of electric mobility systems not just in terms of emissions reduction but also regarding product aesthetics and user experiences [10]. Since mounting of an additional rooftop to place the PV on [8], makes it difficult to the rider to have the same mobility in urban traffic, and placing these ones underneath the rider [9] would be both uncomfortable and less efficient due to shadowing, we deem worthy to bring a design resembling [11], which was practically proven effective, but with enhanced stability due to the proposed mounting of solar panels on both front and rear fenders.

2. MATHEMATICAL MODEL FOR MOTOR DIMENSIONING

The first step for system design is to establish the objectives of the work according to the energy consumption and the performance of the vehicle for individual use. To estimate the power required by this type of vehicles, we have considered that the forces applied to the vehicle are, as represented in Fig. 1, are calculated with the following relations [7].

$$F_a = m \cdot a \quad (1)$$

$$F_g = m \cdot g \cdot \sin\theta \quad (2)$$

$$F_{air} = \frac{1}{2} \rho \cdot C_D \cdot A_f \cdot v(t)^2 \quad (3)$$

$$F_r = m \cdot g \cdot C_R \cdot \cos\theta \quad (4)$$

where: m [kg] – total mass; a [m/s²] – acceleration speed; θ [°] – slope angle; v [m/s] – vehicle speed; F_a [N] – resulting force; F_g [N] – gravitational force; F_{air} [N] – air friction force; F_r [N] – wheels friction force; $\rho = 1.29$ [kg/m³] – air density; A_f [m²] – frontal area of the vehicle; C_D [ND] – air friction coefficient (typically 0.9 for a scooter and 0.8 for a bicycle [7]); C_R [ND] – wheels friction coefficient (usually between 0.008 and 0.014 [7]).

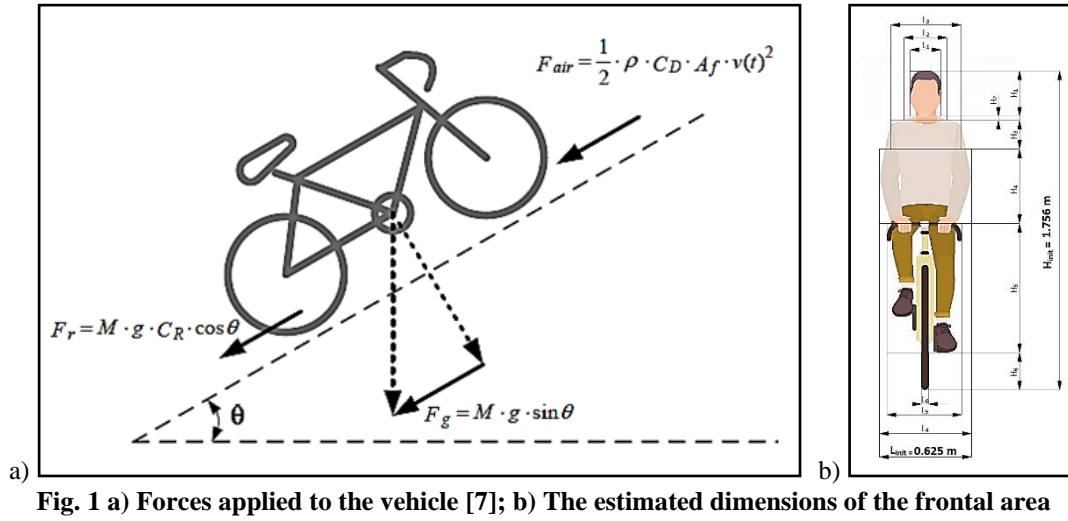


Fig. 1 a) Forces applied to the vehicle [7]; b) The estimated dimensions of the frontal area

From Fig. 1a, we extract the following balance equation:

$$F_a = F_g + F_{air} + F_r \quad (5)$$

We will choose the desired operating parameters in accordance with the desired speed of the vehicle, meaning that we will choose a maximum weight m of 100 kg, a speed v of 4 m/s and an acceleration a of 1 m/s². It is worth mentioning that the EV system was designed to operate at a $\theta_{max} = 10^\circ$. Considering that the vehicle runs with the speed v , the power required by the system [7] can be calculated with the following relation:

$$\begin{aligned} P_{VE} &= P_a + P_g + P_{air} + P_r \leftrightarrow P_{VE} = \\ &= m \cdot a \cdot v + m \cdot g \cdot v \cdot \sin\theta + \frac{1}{2} \rho \cdot C_D \cdot A_f \cdot v^3 + m \cdot g \cdot C_R \cdot v \cdot \cos\theta \end{aligned} \quad (6)$$

Assuming that the vehicle speed is equal to the angular speed ω of wheels with radius R , the torque of the traction system can be estimated as [7]:

$$\begin{aligned} T_{VE} &= T_a + T_g + T_{air} + T_r \leftrightarrow T_{VE} = \\ &= m \cdot a \cdot R + m \cdot g \cdot R \cdot \sin\theta + \frac{1}{2} \rho \cdot C_D \cdot A_f \cdot v^2 \cdot R^3 + m \cdot g \cdot R \cdot C_R \cdot v \cdot \cos\theta \end{aligned} \quad (7)$$

The chosen operating parameters for calculating the power of the EV according to equations (1)-(7) are displayed in Table 1 below (where R is the radius of the bike wheel).

Table 1. Pre-established parameters for calculating the power of the EV system

m [kg]	a [m/s ²]	g [m/s ²]	$\sin(10^\circ)$ [ND]	$\cos(10^\circ)$ [ND]	ρ [kg/m ³]	C_D [ND]	C_R [ND]	A_f [m ²]	v [m/s]	R [m]
100	1	9.8	0.17	0.98	1.29	0.8	0.01	0.76	4	0.3

In order to determine the frontal area of the assembly, a rough estimation was required. We considered the case of an average male, with the height H_{mit} of 1.765 m and a shoulder length L_{init} of 0.625 m. The total frontal area was divided in six smaller areas.

The estimations that were made for A_1, A_2, A_3, A_4, A_5 and A_6 are presented in

Table 2. The areas were calculated based on the dimensions in Fig. 1b ($A_n = L_n \cdot H_n$).

Table 2. Pre-established parameters for calculating the power of the EV system

A_1 [m ²]	A_2 [m ²]	A_3 [m ²]	A_4 [m ²]	A_5 [m ²]	A_6 [m ²]
0.045	0.008	0.096	0.248	0.351	0.013

Given these parameters and using equations (1)-(6), we were able to calculate the necessary power for the EV, but also the forces applied to our system. The results are presented in Table 3. In doing so, we can determine that, according to the data preestablished in Table 1, a motor with a power of 3.5 kW can be used.

Table 3. The resulting forces, motor power and torque of the EV system

F_a [N]	F_g [N]	F_{air} [N]	F_r [N]	P_{VE} [W]	T_{VE} [Nm]
100	166.6	6.27	9.6	1129.91	91.67

3. THE HARDWARE COMPONENTS

3.1. The motor

For this study, a brushless DC electric motor (BLDC motor) with the power of 3500 W was considered (Fig. 2). The 3500 W BLDC 125/6D MOTOR has a total length of 225 mm, flange size of 140 mm, a mounting diameter of 50 mm and a weight of 12.5 kg.



Fig. 2 The 3500 W BDLDC 125/6D Motor [12]

The motor will be attached to the front on the EV and in doing so, we are ensuring enough power to overcome the F_a , F_g , F_{air} and F_r forces established in Section 2.

3.1. The battery

In choosing the battery for this study, the ergonomic productivity of the system was one of the aspects that need to be prioritized. Bearing this in mind, we have chosen a battery from a series that specializes in electrical bike batteries. The 24 V ODM Series Aluminum Case Model KL2497 battery [13] in Fig. 3a was considered, of $89 \times 87 \times 232$ [mm] and weighting 2 kg. The main components of a battery pack for an electric bicycle are shown in Fig. 3b.

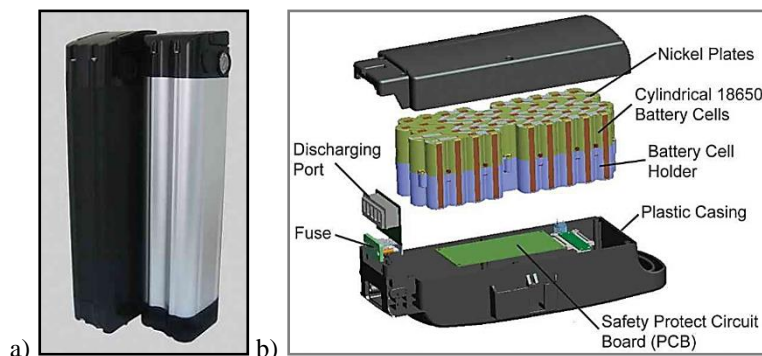


Fig. 3 a) 24V ODM Battery Model KL2497 [13]; b) Exploded view of a battery pack [13]

There are a few commonly used places for battery mounting (Fig. 4), offering accessibility and at the same time providing minimum of inconvenience for the cyclist. The mounting place will be established subsequently, after a proper computation of the weight distribution of the other components.



Fig. 4 Possible mounting places for the battery [13]

3.2. The solar panels

Another main concern for the assembly is that it should be easy to use in urban areas, which implies that the total width of the system should be kept at a minimum. When choosing the PV panels, we took into consideration the pre-determined L_{int} in Section 2. Therefore, the Sunpal SP50M-36 Monocrystalline Solar Panels [14] were considered, each panel having a peak power value of 50 W and a maximum voltage of 18.32 V.

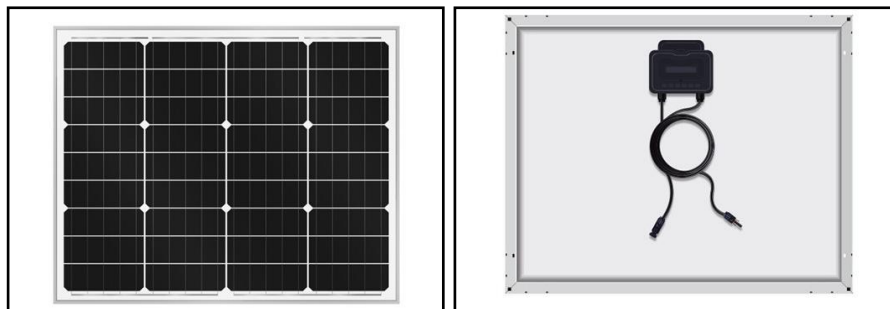


Fig. 5 The SP50M-36 Monocrystalline Solar Panel [14]

4. ESTABLISHING THE INSTALLATION PLACE OF PHOTOVOLTAIC PANELS

When designing the EV system, two PV panels will be used for storing the solar energy into the battery. Even though mounting the panels on the top tube or frame of the bike might seem the easiest and sturdiest option (Fig. 6a, Fig. 6b), the installation would only obscure the light to properly reach the PVs. Furthermore, it will represent an inconvenience for the user.

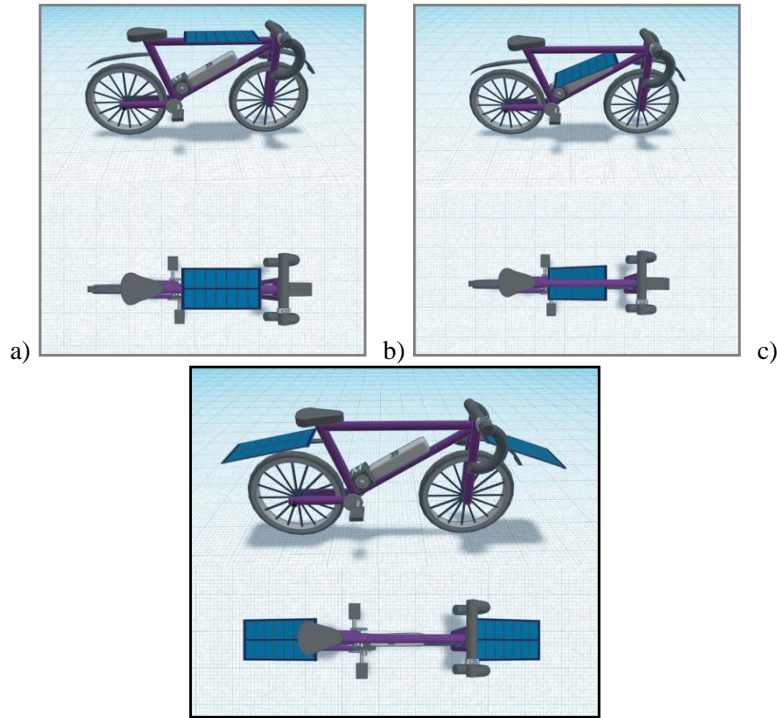


Fig. 6 Placing the PV panels on the top tube (a) or frame of the vehicle (b); Placing the PV panels on the fenders of the vehicle (or with a custom-made support) (c)

Since the weight of the panels may cause collisions of mechanical nature, this will influence the way of mounting them. The panels will be placed either on the fenders of the wheels, or with a custom-made support, as presented in Fig. 6c.

5. BATTERY CHARGING TIME VIA SOLAR PANELS

With the help of professional and reliable websites [15-19], we can calculate the battery charging time. After introducing the initial data known from the data sheets of the chosen components, we calculated the charging time of the battery using the two solar panels. It is worth mentioning that the calculations hereinafter for the charging time were realized for a Lead Acid type battery and an MPPT (Maximum Power Point Tracking) type of solar charge controller.

We know that one solar panel has a power $P_{\text{solar_panel}}$ of 50 W and a voltage $U_{\text{solar_panel}}$ of 18.32 V, while the battery has a voltage U_{battery} of 24 V and a capacity Q_{battery} of 8.8 – 11.6 Ah (we consider $Q_{\text{battery}} = 10$ Ah). Knowing these, we will calculate the charging time in six steps, keeping in mind that we are using two solar panels electrically connected in series.

- a) Calculating the battery capacity:

$$C_{\text{battery}} = U_{\text{battery}} \cdot Q_{\text{battery}} = 240 \text{ Wh} \quad (8)$$

Estimating how much of the battery's power capacity is discharged by multiplying the battery power capacity with battery depth of discharge (*DoD*). A *DoD* of 100% is assumed since the ODM Series are lithium batteries [15]:

$$C_{\text{discharge}} = C_{\text{battery}} \cdot \text{DoD} = 240 \text{ Wh} \quad (9)$$

- b) Calculating the amount of energy required to fully charge the battery after factoring in losses during charging, by dividing the discharged battery power capacity by the charge efficiency factor (lead acid: 85%; lithium: 99%):

$$E_{full_charge} = \frac{C_{discharge}}{\eta_{efficiency_battery}} = 242.42 \text{ Wh} \quad (10)$$

- c) Estimating the solar power output by multiplying the solar panel power with charge controller efficiency (PM: 75%; MPPT: 95%):

$$P_{solar_output} = P_{solar_panel} \cdot \eta_{efficiency_battery} = 95 \text{ W} \quad (11)$$

- d) Calculating the solar power output by taking into account the system losses (14.08% is considered a default value for system losses, according to The National Renewable Energy Laboratory's PVWatts Calculator [20]):

$$P_{adjusted} = P_{solar_output} \cdot (100\% - 14.08\%) = 81.62 \text{ W} \quad (12)$$

- e) Estimating the charging time by dividing the amount of energy required to fully charge the battery (in watt hours) by the adjusted solar power output:

$$t_{charge} = \frac{E_{full_charge}}{P_{adjusted}} = 2.96 \text{ h} \quad (13)$$

The system losses account for performance losses one would expect in a real system that are not explicitly calculated by the PVWatts model equations. The default value for the system losses of $\eta_{syst} \cong 14\%$ is based on the categories in Table 4, and is calculated with relation (13) [20].

$$\eta_{syst} = 100 \cdot [1 - (1 - \eta_s) \cdot (1 - \eta_{sh}) \cdot (1 - \eta_m) \cdot (1 - \eta_w) \cdot (1 - \eta_c) \cdot (1 - \eta_l) \cdot (1 - \eta_n) \cdot (1 - \eta_a)] \quad (14)$$

Table 4. Default values for the system loss categories [20]

Category	Symbol	Default Value [%]
Soiling	η_s	2
Shading	η_{sh}	3
Mismatch	η_m	2
Wiring	η_w	3
Connections	η_c	0.5
Light-Induced Degradation	η_l	1.5
Nameplate Rating	η_n	1
Availability	η_a	3

6. RESULTS

The results can be seen in the two subsequent figures. The parameters and mathematical relations discussed previously were introduced into Matlab Simulink Online using mathematical operations and introducing the numerical values via constant blocks for computing the power required by the system (Fig. 7a), as well as the torque of the traction system (Fig. 7b). As calculated with the software, we can also charge the 24 V battery in 2.96 h of direct sunlight, which would be the ideal case whether the vehicle is being used.

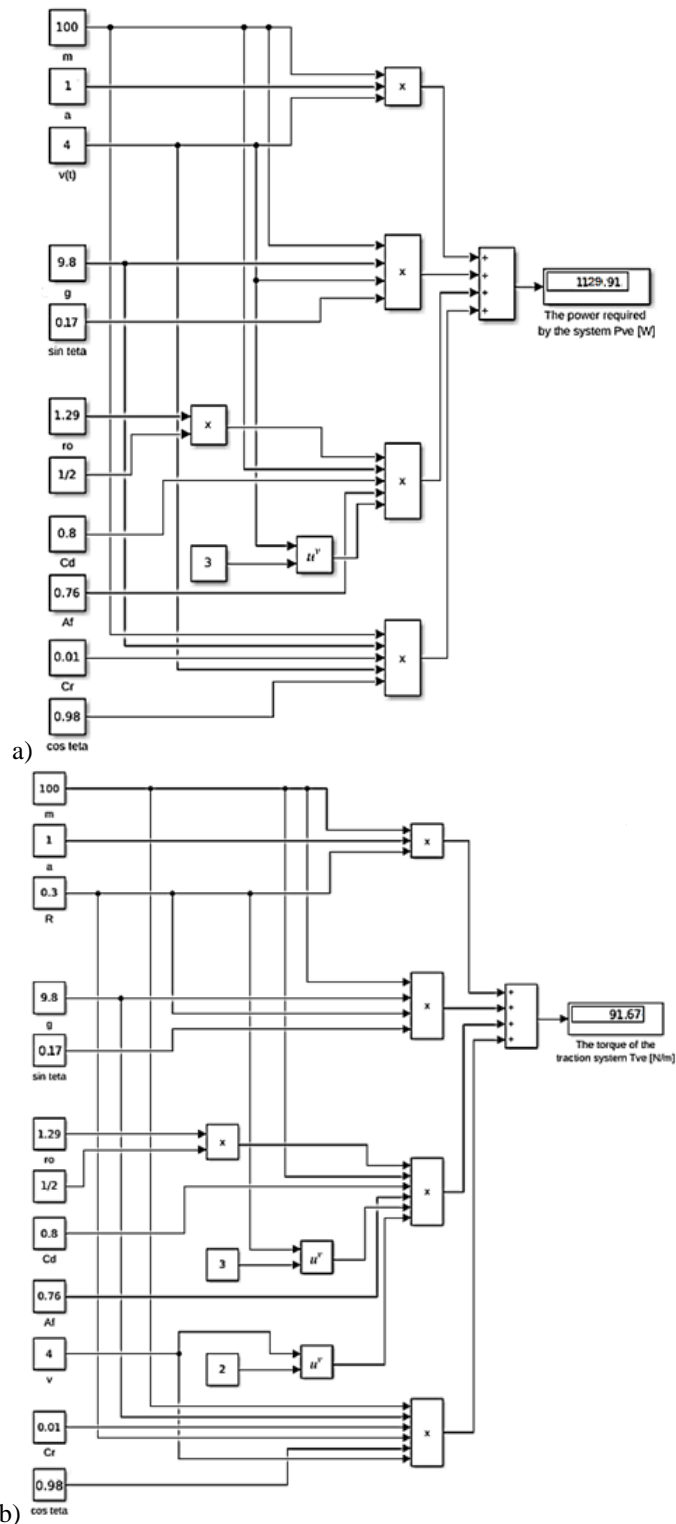


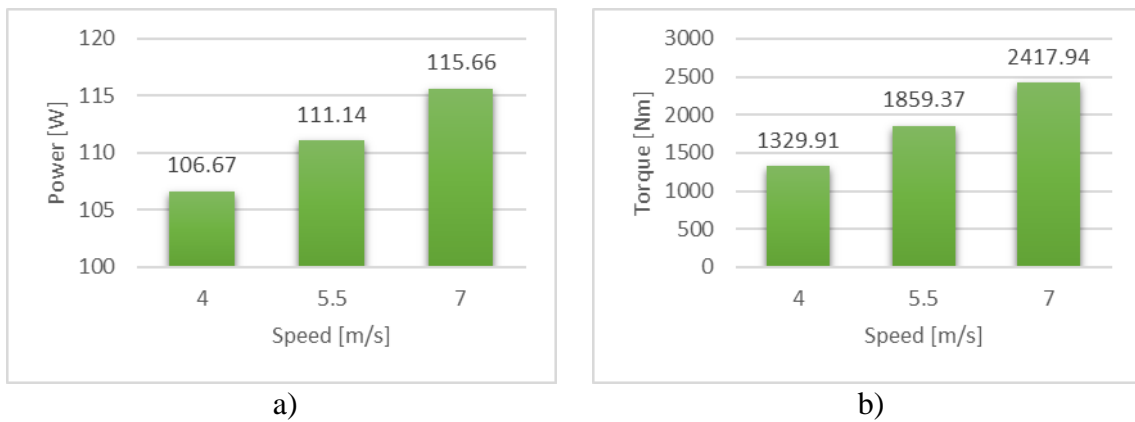
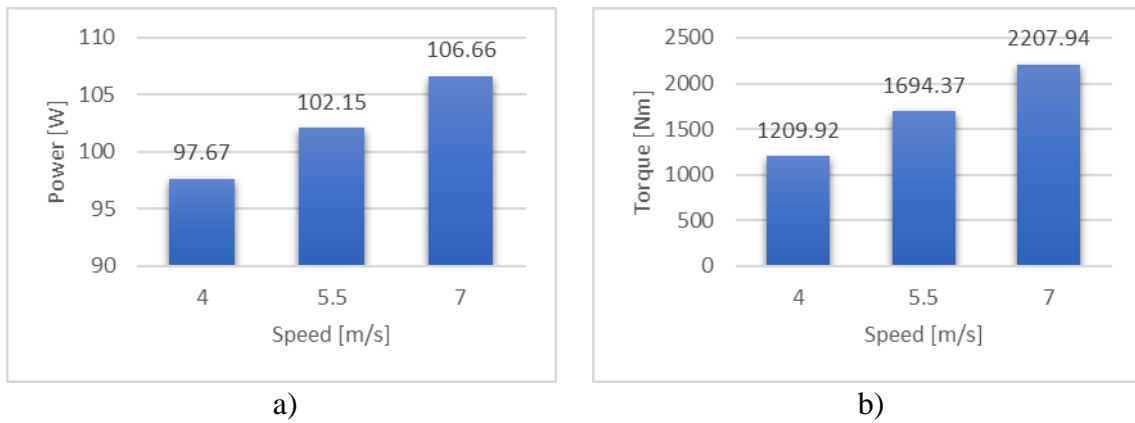
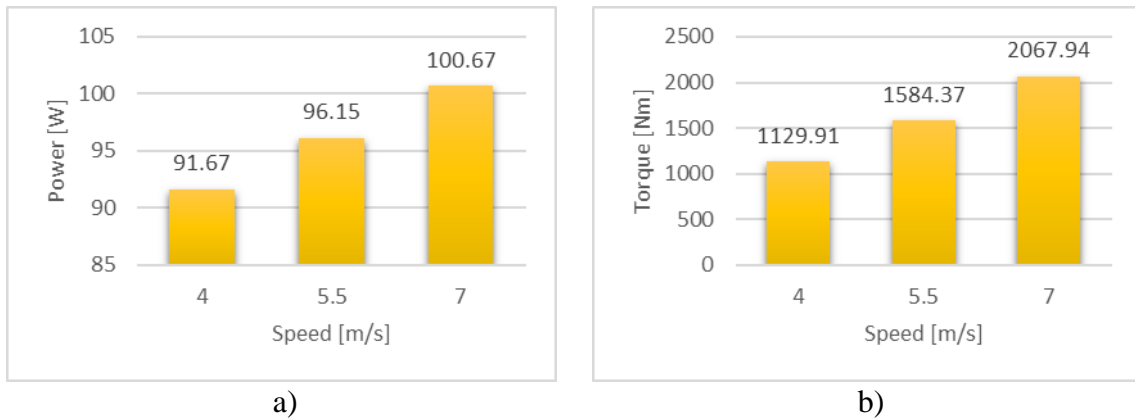
Fig. 7 The Simulink models for the required power, P_{VE} (a) and torque of the traction system, T_{VE} (b)

Keeping in mind the pre-established parameters discussed in the mathematical model for the motor dimensioning and the weight of each hardware component, we conclude that at the current state of the study, in order of achieving the best performance for our system, the user should weight at around 61 kg, given by the rough estimations of the EV's weight displayed in Table 5.

Table 5 The estimated weight of the EV

<i>Electric Motor</i> [kg]	<i>Battery</i> [kg]	<i>PV Panel</i> [kg]	<i>Auxiliary Equipment</i> [kg]	<i>Bicycle</i> [kg]
12	2	6.5	1.5	10

The charts in the figures hereinafter aim to present the power required by the system in order to provide the traction torque, calculated for three stages of acceleration, namely 1 m/s^2 (Fig. 8), 1.2 m/s^2 (Fig. 9) and 1.5 m/s^2 (Fig. 10) respectively.



7. CONCLUSIONS

In this study it has been established that, for our pre-determined parameters of the electric vehicle with PV panels, a motor with a power of 3.5 kW is required, alongside a 24 V battery and two 50 W solar panels, those conditions being applied for an average male, with a height of 1.765 m and estimating the total weight of the system and the user reaching 100 kg.

It has also been established that, since the vehicle will be used in urban areas, the maximum slope angle that the calculations were executed was $\theta_{\max} = 10^\circ$, while being able to maintain an acceleration of 1 m/s^2 and a maximum speed v of 4 m/s, with the exemplification of the power and torque necessity of the system if the maximum speed of the vehicle would have been increased to 5.5 m/s and 7 m/s.

The optimal placement of the PV panels has been decided in Section 4. Seeing that the solar cells should collect the maximum amount of solar radiation, they have been placed on the fenders of both wheels of the bike. Another option would be to use custom-made mounts for the solar panels in order to avoid mechanical failures caused because of the weight of the PVs.

Using available resources, we were able to calculate the charging time t_{charge} of the system, at around 3 hours. Charging a 24 V battery with two 50 W solar panels is possible, however, we will need a solar charge controller to regulate the voltage and prevent overcharging. Since the maximum power voltage of a solar panel is 18.32 V per panel, it may not be sufficient to fully charge a 24 V battery, so we will have to consider additional panels or a different battery.

Future research will focus on a weight distribution analysis, as well as simulations regarding the power produced by the photovoltaic module and battery charging time. The required circuitry and a voltage boost converter will also be addressed. Since the motor power corresponds to a scooter rather than a bicycle, recalculating the power required without the starting part will be considered, as the starting is realized by pedaling. The proposed design is a starting point that needs a lot of improvement and work, this being the reason behind choosing low-cost components regarding a future prototyping of the solution, without funding.

REFERENCES

- [1] K. Martens, *The bicycle as a feeding mode: experiences from three European countries*, Transportation Research Part D: Transport and Environment, 9, 4, pp. 281-294, 2004. DOI: [10.1016/j.trd.2004.02.005](https://doi.org/10.1016/j.trd.2004.02.005).
- [2] G. Apostolou, A. Reinders and K. Geurs, *An Overview of Existing Experiences with Solar-Powered E-Bikes*, Energies, 11, 8, p. 2129, 2018. DOI: [10.3390/en11082129](https://doi.org/10.3390/en11082129).
- [3] P. Dumitru, T. Radu and O. Marian, *Photovoltaics changing the face of the big cities-electric bicycles supplied by solar panels*, 2014 49th International Universities Power Engineering Conference (UPEC), Cluj-Napoca, Romania, 2014, pp. 1-4. DOI: [10.1109/UPEC.2014.6934776](https://doi.org/10.1109/UPEC.2014.6934776).
- [4] A. Solanki, S. Reddy and K. Kishor, *Modeling, Simulation and Performance Analysis of Solar PV System*, International Journal for Modern Trends in Science and Technology, 7, 9, pp. 264-272, 2021. DOI: [10.46501/IJMTST0709043](https://doi.org/10.46501/IJMTST0709043).
- [5] A. Muetze and Y. Tan, *Electric bicycles - A performance evaluation*, IEEE Industry Applications Magazine, 13, 4, pp. 12-21, 2007. DOI: [10.1109/MIA.2007.4283505](https://doi.org/10.1109/MIA.2007.4283505).
- [6] N. Hatwar, A. Bisen, H. Dodke, A. Junghare and M. Khanapurkar, *Design approach for electric bikes using battery and super capacitor for performance improvement*, 16th International IEEE Conference on Intelligent Transportation Systems (ITSC 2013), The Hague, Netherlands, 2013, pp. 1959-1964. DOI: [10.1109/ITSC.2013.6728516](https://doi.org/10.1109/ITSC.2013.6728516).
- [7] D. Sousa, P. Costa Branco and J. Dente, *Electric bicycle using batteries and supercapacitors*, 2007 European Conference on Power Electronics and Applications, Aalborg, Denmark, 2007, pp. 1-10. DOI: [10.1109/EPE.2007.4417425](https://doi.org/10.1109/EPE.2007.4417425).
- [8] H. Patoding, R. Palebangan and M. Silolongan, *Electric bicycles with solar panels*, IOP Conference Series: Materials Science and Engineering, 1088, p. 012106, 2021. DOI: [10.1088/1757-899X/1088/1/012106](https://doi.org/10.1088/1757-899X/1088/1/012106).
- [9] V. Raut, V. Gund, A. Thorat and Y. Funde, *Design and Manufacturing of Variable Speed Solar Power Bicycle*, in International Journal on Recent and Innovation Trends in Computing and Communication (Special Issue ICIIME 2017), 5, 6, pp. 1248-1252, 2017.
- [10] A. Sierra and A. Reinders, *Designing innovative solutions for solar-powered electric mobility applications*, Progress in Photovoltaics: Research and Applications, 29, 7, pp. 802-818, 2020. DOI: [10.1002/pip.3385](https://doi.org/10.1002/pip.3385).

- [11] M. Toll, *This solar-powered electric bicycle is making a 6,500-mile loop around US*, Electrek, 2021. <https://electrek.co/2021/10/19/this-solar-powered-electric-bicycle-is-making-a-6500-mile-loop-around-us/>.
- [12] 3500watt/3.5kW 48/72V 3000rpm BLDC Motor, indiamart.com, 2022. <https://www.indiamart.com/proddetail/3500watt-3-5kw-48-72v-3000rpm-blcd-motor-17465529373.html>.
- [13] PortaPower Ltd., *Electric Bicycles Battery*. Portapower.com, 2022. <http://portapower.com/files/pdf/e-Bike-Battery.pdf>.
- [14] *China Customized 50W Solar Panel Manufacturers, Suppliers, Factory - SUNPAL*, Sunpal Power Co., Ltd. <https://www.sunpal-solar.com/solar-panel/customized-solar-panel/50w-solar-panel.html>.
- [15] *Solar Panel Charge Time Calculator*, Footprint Hero. <https://footprinthero.com/solar-panel-charge-time-calculator>.
- [16] *Solar Ebike Systems - Learn*, Ebikes.ca. <https://ebikes.ca/learn/solar.html>.
- [17] *How To Make a Solar Powered Electric Bike*, GearLab. <https://www.outdoorgearlab.com/expert-advice/how-to-make-a-solar-powered-electric-bike>.
- [18] *Can You Charge an Ebike with a Solar Panel? - Powmr*, Powmr.com. <https://powmr.com/blog/can-you-charge-an-ebike-with-a-solar-panel/>.
- [19] *Solar Panel Charging Calculations of a Battery (Figures You Need) - 2022*, Sol Voltaics: Solar Panel Information, 2022. <https://solvoltaics.com/solar-panel-charging-calculations/>.
- [20] *PVWatts Calculator*, Nrel.gov, 2019. <https://pvwatts.nrel.gov/index.php>.

Disclaimer/Publisher's Note: The statements, opinions and data contained in all publications are solely those of the individual author(s) and contributor(s) and not of COMOTI or the editor(s). COMOTI and/or the editor(s) disclaim responsibility for any injury to people or property resulting from any ideas, methods, instructions or products referred to in the content.

SIV FOR AN RTJ, USING A PIV COMMERCIALLY AVAILABLE POST-PROCESSING SOFTWARE

Emilia-Georgiana PRISĂCARIU ¹

Received: 09.05.2023
Accepted: 22.05.2023
Published: 14.07.2023

Copyright: The article is an Open Access article and it is distributed under the terms and conditions Creative Commons Attribution (CC BY) license (<https://creativecommons.org/licenses/by/4.0/>).



ABSTRACT: Recent developments in the field of schlieren image velocimetry (SIV) are presenting an increase in measurement accuracy due to the higher computational power available. The present paper aims at providing data regarding the velocity profiles of an encapsulated, round, turbulent exhaust jet. The data obtained from an FFT-based commercial cross-correlation solution is analysed, together with the direct cross correlation of the schlieren images. The methods applied here yield results which follow the classical trend regarding velocity distributions. An investigation regarding how the software settings affect the results, is conducted. Working hypothesis are formulated and future work suggestions regarding the improvement of the measurement's accuracy are made.

KEYWORDS: SIV, PIV, cross correlation, FFT, DCC, measurement accuracy.

NOMENCLATURE

Al=Aluminum
DCC= direct cross-correlation
EDH= electrohydrodynamic
EFL= effective focal length
FFT = Fast Fourier Transform
fps=frames per second
H=hidrogen
O= oxygen
PIV=Particle mage velocimetry
PTV=Particle Image Tracking
Px=pixel
RGB= color channels (Red, Green, Blue)
ROIs=regions of interest
RPC=robost phase correlation
RTJ= round turbulent jet
SIV=schlieren image velocimetry
SNR=signal to noise ratio

¹ Romanian Research and Development Institute for Gas Turbines COMOTI

1. INTRODUCTION

SIV has been known to represent, in the last decades, an alternative to the most commonly used Particle image Velocimetry (PIV) method, which uses particles introduced in the flow as tracers and provides velocity data of the whole 2D/3D flow field. The main issue with PIV is that it assumes that the tracer particles introduced into the flow, follow the flow perfectly. Seeding can be challenging or even impossible in different flow media, such as compressible flow [1] or electrohydrodynamic (EDH) flows [2], [3]. PIV measurements in turbulent or supersonic flows are prone to return faulty results unless considerable actions regarding the following issues are taken. These errors, in the case of supersonic flows, can be caused by particle slip in the areas where shock waves develop, improper seeding mechanisms, or the inadequate particle distribution within the studied flow [4].

These issues caused a spike of interest in SIV, which is non-intrusive and uses the flow's fine turbulent elements to describe its motion. Eddies formed within the flow replace the tracer particles used in PIV. The small eddies (which have proper dimensions to be considered as tracking elements, and therefore can be investigated with the intended SIV method) length scale decrease with the Reynolds number, which becomes very important in SIV measurements. These self-seeded images are recorded with a short time-delay to be further cross-correlated, yielding information about the flow field [5].

One of the first authors to apply high-speed imaging for SIV at the 100.000 kHz magnitude is Fu [6], who used the recording speed of to extract velocity field information, with help from the digital particle image velocimetry algorithm, developed at the end of the twentieth century [5]. Flow field information has been computed by using the background oriented schlieren (BOS) method, by Raffel [7], Scarano [8], Elsinga [9]-[10] and Kindler [11]. The idea of using a commercially available software to post-process SIV images was confronted by Jonassen and Settles and applied to an axisymmetric helium jet and a 2D supersonic turbulent boundary layer [12]. The study concluded that the "schlieren PIV" technique yields valid velocimetry data for a 2D compressible turbulent boundary layer and an axisymmetric turbulent helium jet in air. The center plane velocity data for the round jet was extracted by performing the Invers Abel Transform, given the assumption that the velocity has a path-integrated character. At the present time, this hypothesis has been disproved by Schmidt and Page [13], which successfully showed that schlieren velocity fields are rather path-averaged, than line integrated. The "schlieren PIV" experiment conducted by Johansen and Settles had the evolutionary scale of the turbulent eddies larger than the separation time between the recorded frames, allowing proper sampling of the turbulent elements. It showed a very good premises for future system optimization, starting with a simple set-up which used classical schlieren optics coupled with a commercially available software. [5] performs a statistical assessment of three different SIV set-ups, comparing the vertical and horizontal knife-edge schlieren methods with the shadowgraph method. The test case is a high velocity helium jet (Mach 0.3-0.6), whose images are post processed with the robust phase correlation algorithm (RPC) [14], for its enhanced measurement capabilities, reduced signal to noise ratio (SNR), peak locking, etc. The schlieren methods deployed used two SIV cameras to account for the high velocity of the flow, testing the flow for two different Reynolds numbers. The study concluded that the horizontal knife-edge (with a cut-off of 40%) and the shadowgraph method yielded results in good agreement with the PIV measurements, while the vertical cut-off performed poorly and provided inconsistent signal content. The method applied here was concluded to be adequate for 2D turbulent flows.

The present paper investigates the flow field velocity of an $H_2 - O_2$ exhaust jet, captured by means of schlieren, with a high-speed camera. The jet analyzed is formed out of water vapors after the chemical reaction took place. The investigated jet is not a chemically reactive jet.

The images of the jet's plumes are post processed with PIVlab [15]. The purpose of the paper is to help optimize a visualization method to yield quantitative results regarding the encapsulated exhaust jet, without intruding the phenomena. The data regarding the velocimetry profiles yielded by SIV can provide insight into the working parameters of the thruster that generates the analyzed exhaust jet. More information about the development of the micro thruster generating the investigated exhaust jet can be found in [16].

2. EXPERIMENTAL SETUP

The images of the exhaust jet have been recorded with a schlieren system which makes use of 2 identical parabolic mirrors, a high-speed camera and an LED as a light source. Their specifications can be found in Table 1.

As mentioned before the jet forms in an enclosure meant for vacuum testing, but for this study the images were recorded with the jet dispersing in air. Given certain space limitations, the classical Z-type schlieren configuration was adapted to form a U-turn, as it can be observed in Fig. 1. The glass windows of the vacuum chamber have a smaller diameter in comparison to the diameter of the parabolic mirrors.

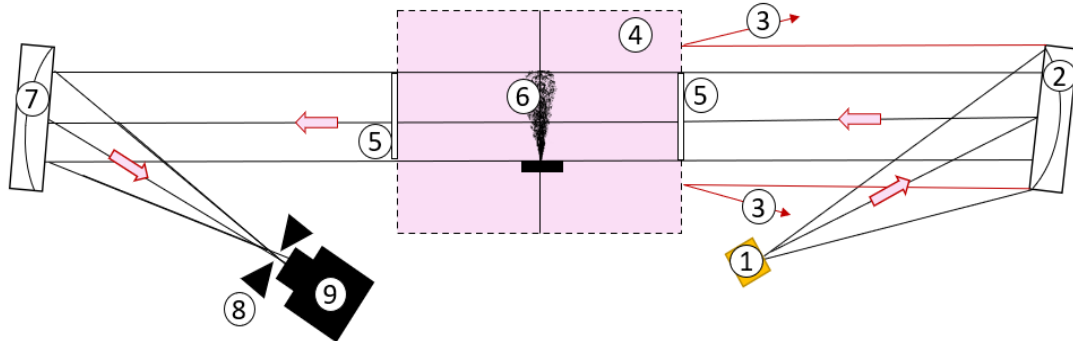


Fig. 1 Schlieren experimental set-up: 1- light source; 2- first parabolic mirror; 3- light rays deflected by the vacuum chamber's casing; 4- vacuum chamber; 5- vacuum chamber glass windows; 6- axisymmetric exhaust jet; 7- second parabolic mirror; 8- iris diaphragm; 9- high-speed camera.

The circular knife-edge cut-off has been chosen specially to avoid having intermittent evolution of the tracking elements, given the fact that the horizontally and vertically placed knife cut-offs work by eliminating x or y density gradients.

A standard 50% cut-off has been applied, to account for both high and low-density areas of the jet. In literature, this cut-off level is considered to represent a moderate amount [17].

The light rays propagate from the light source and are uniformly distributed onto the parabolic mirror, which projects them onto the vacuum chamber's outer casing. Given the dimension of the glass windows, some of them are reflected back, while others continue to collimate against the second parabolic mirror. The second parabolic mirror is turned in a U shape to focus the rays onto the circular knife-edge, oriented in the video camera's direction.

The thruster pulse was 0.5 seconds, and the exhaust plume was recorded on its entire duration. The frames used to conduct the studies were assumed to be taken when the jet was fully developed.

Table 1. Specifications of the equipment used for schlieren image acquisition

No.	Equipment	Type	Important specifications
1	High speed camera	Phantom Veo 710L	Recording speed 33.000 fps at the resolution of 512x384 pixels
2	2 twin parabolic mirrors	Edmund Optics	Al-plated, 25cm diameter, EFL=1524mm
3	Knife-edge	Iris diaphragm	Circular cut-off, 1.5mm diameter
4	Light source	Singular LED	3mm, equipped with small biconvex mirror Wavelength 440 nm Output power: 85 lumens
5	Data acquisition system	Laptop	Alienware m15 Processor: intelCore i7

3. SIV IMAGES PRE-PROCESSING

The raw images recorded presented a high-level of natural convection. At the exit of the jet, pressure waves can be observed. These are propagating for a couple of frames as seen in Fig. 2 a), after which they hit the vacuum chamber casing and they return Fig. 2 b), interfering with the schlieren background.

However, the image of the pressure waves is only used as an example to help with the understanding of how the natural convection is amplified by the vacuum chamber's casing which doesn't allow a fast temperature dispersal either.

The studied jet is considered as fully developed and at nominal working regime when the analyzed images are recorded. The pressure waves are therefore not present in the analyzed image sequence and the study of their forming mechanism goes beyond the goals of the present paper.

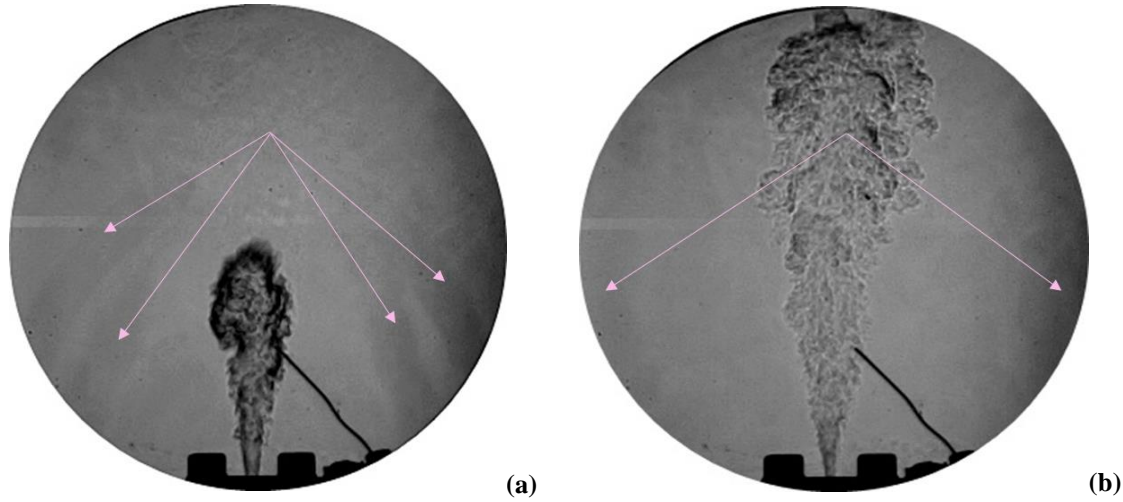


Fig. 2 Schlieren raw images with enhanced contrast: (a) dispersing pressure shockwaves at the thruster's exit; (b) weak pressure waves reflected by the vacuum chamber's casing.

The images were post processed before being introduced in the cross-correlation algorithms, for several reasons. Firstly, the background needed smoothing. Eliminating the elements that don't belong to the jet but can be found in the near vicinity is important. Having "rogue" elements can affect the overall accuracy of the tracking mechanism. Despite the schlieren camera's capabilities of recording at very high speeds, while keeping the RGB character of the image, the image of the jet remains a schlieren image, in which the main colors represented will be white to black, going through as many shades of gray as the camera's sensor is capable of rendering and as many as the number of density variations found in the experiment. In this case, the camera is a 24-bit camera, hence it can render up to 2^{24} shades of gray. Given the fact that the images will be cross correlated later, their binarization must be avoided, doing so causes data regarding subpixel interpolation to be lost. Most high-speed cameras present a green tint when the light entering its sensors has low intensity. This is a saturation issue and is preferable to remove it by gray scaling the images rather than binarizing them. Other operations taken into account after performing the background smoothing and gray scaling can be adjusting the image size to only include the phenomena and designing a special mask to cover up the rest of the physical set-up. In the case of the commercially available software (PIVlab), the mask option is available, allowing customized coverage, otherwise, it should be created to help reduce spurious vectors appearing in regions outside of the investigated ROIs. Fig. 3 is presented below to serve as a visual comparison of the preprocessing effort.

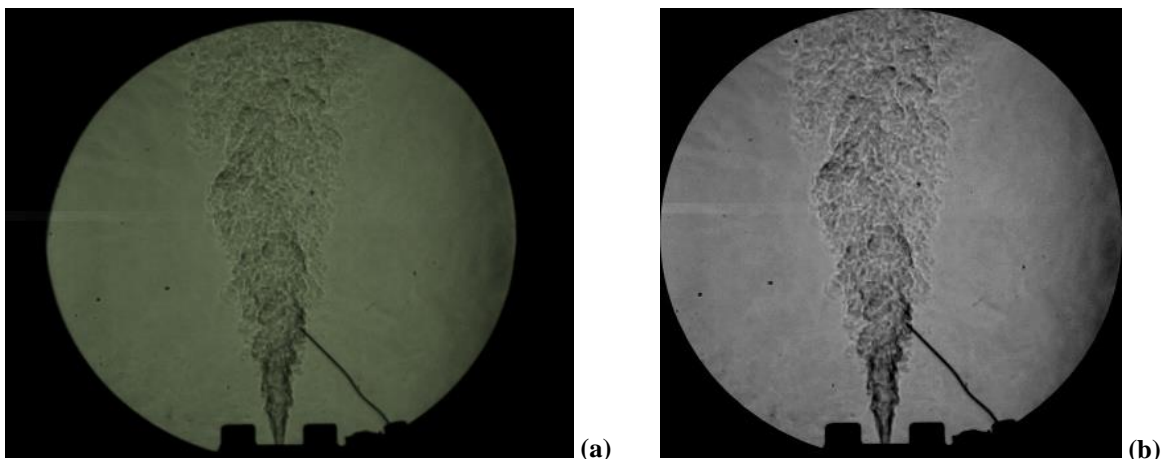


Fig. 3 Schlieren frames of the exhaust jet: (a) before and (b) after pre-processing

4. PIVlab IMAGE CROSS-CORRELATION

Image cross-correlation has been related to the PIV method and the principle's basis was established and described by many fundamental papers. Fundamental studies in the PIV domain, followed the work of Meynart [18], are represented by Adrian [19], Westerweel [20] and Willert [21]. The cross correlation principle has been described by a numerous amount of authors, in various forms, but the fundamentals of the statistical process involved in the cross correlation principle is highlighted in the outstanding works of Adrian [22] and Raffel *et al.* [23].

A compact explanation behind the cross-correlation principle and the correlation method, is found in [24]. As the present paper presents an FFT cross-correlation, achieved by PIVlab, the usefulness of applying the classical FFT standard functions [25] is further explained.

4.1. The cross-correlation principle

Let C be considered the particle concentration per unit of volume, and being randomly distributed. If it's randomly distributed, we assume the k to be the number of particles situated in the volume V . Therefore, the distribution follows the Poisson rule:

If Δz_0 is considered to be the thickness of the light sheet used for acquiring the planar PIV images, the mean distance between two neighbor and a nearest particles in the planar projection of the light sheet can be expressed as:

$$r_n = \frac{1}{2} (C\Delta z_0)^{-1/2} \quad (2) [24]$$

If we consider L_I to be the square interrogation area and M^2 the total image surface, the image density will be defined as:

$$N_I = \frac{C\Delta z_0 L_I}{M^2} \quad (3) [24]$$

If there are many particles per interrogation area ($N_I = \text{large}$), then a good estimation of the statistical displacement can be achieved. Unlike PTV, where no statistical displacement can be determined, as the goal of the technique is to individually follow particles, in the case of PIV, if a structure moves as a whole, the correlation peak will be situated at the shift corresponding to the translation [24].

The correlation method can be simplified by considering the correlation between two functions, $f(x)$ and $g(x)$. The correlation between these two functions is described by (4).

$$f * g = C_{fg}(\Delta x) = \int_{-\infty}^{+\infty} f(x)g(x + \Delta x)dx \quad (4) [24]$$

The correlation of the functions is, therefore, the product of the functions $f(x)$ and $g(x)$, with $g(x)$ shifted on a Δx distance. For each Δx shift, a new value of the correlation is obtained.

If one further equals $f(x) = \delta(x - x_f)$ and $g(x) = \delta(x - x_g)$, their correlation can will be $C_{fg}(\Delta x) = \delta(x - x_{fg})$. From this, the correlation peak can be extracted:

$$x_{fg} = x_g - x_f \quad (5) [24]$$

From (5) it can be determined that the correlation peak is found at x_{fg} , with the correlation value of 0 everywhere else.

As described above, the correlation of the two functions must be calculated. If each function has N points, the correlation evaluation has N^2 operations. For example, for a 2D plane, there will be a number of $N \times N$ collocation points, and the number of operations will become N^4 . The number of operations can increase significantly, and this is the main reason behind the use of FFTs.

The explanation behind the use of FFTs is further found in the analysis of the correlation theorem. Assume k as a number of wavelength, and as a function of λ .

$$k = 1/\lambda \quad (6) [24]$$

Then, the correlation theorem can be written as:

$$C_{fg} = \int_{-\infty}^{+\infty} f(x)g(x + \Delta x)dx \quad (7) [24]$$

From (7), by applying the inverse Fourier transform (\mathcal{F}^{-1}), the correlation theorem becomes:

$$C_{fg}(\Delta x) = \mathcal{F}^{-1}[F(k)G(k)] \quad (8) [24]$$

For 2D, the values of x and k can be replaced by the vector equivalents. If an FFT is applied on a 2D discrete set of data, the correlation becomes $\mathcal{O}(2N^2 \log_2 N)$, which presents a reduction factor of 256/3, for a value of $N=32$, compared to the previous $\mathcal{O}(N^4)$ solution.

$$P(k, v) = \frac{(cv)^k}{k!} e^{-cv} \quad (1) [24]$$

4.2. SIV images post-processing with PIVlab

PIVlab [15] is a commercially available application, which can be installed within the *Matlab* software. It represents a good alternative for PIV images post-processing. Most PIV studies rely on in-house developed software whose functions can be less optimized than the ones performed by a commercial software, given the less hours invested into its development.

PIVlab offers the possibility of analyzing the PIV images using 3 options: direct correlation, FFT correlation and ensemble. For the post processing of the SIV images studied in this paper, the FFT option has been selected. A pair of two consecutive images has been analyzed in 3 different sessions. The sessions' settings are presented in Table 2.

For each cross-correlation session, a series of dimensions for the interrogation window area must be provided. In classical PIV, the interrogation windows and the interrogations steps are defined as squares.

The interrogation windows are set to be scanned with the interrogation step, resulting into a correlation peak, which creates the displacement vector.

Scanning in the vicinity of the step area (hence, in the interrogation window), represents a faster way to determine the correlation peak than the method of scanning the entire image. One pass refers to a single interrogation window, scanned by a single step. As mentioned in Table 2, the sessions applied here are defined by 3, 2 and respectively 1 pass.

The number of the displacement vectors resulted is related more to the dimension of the step and the interrogation window, and less to the number of the passes, as it can be observed in Fig. 4, where image (a) contains the same amount of vectors as image (c), because the input of the last pass is the same (16x8), while image (b) contains a larger vector sample, due to the smaller pass setting (8x4).

The subpixel interpolator is a mechanism which determines the correlation peak with subpixel precision. The principle of the Gaussian 2-3-point fit implies that the subpixel precision is achieved by fitting a one-dimensional Gaussian function to the integer intensity distribution of the correlation matrix for both axes independently [15].

Table 2. Settings used in the PIVlab post processing sessions.

Session no.	Number of passes	Interrogation window area vs. interrogation step	Other specifications, available for all of the sessions
1	3	64x32; 32x16; 16x8	Subpixel interpolator: Gauss 2x3-point Magnification factor: 1px = 0.00054m Coordinates: x increases towards right y increases towards top Contrast stretch - active
2	3	32x16; 16x8; 8x4	
3	2	32x16; 16x8	
4	1 (DCC)	16x8	Raw image analysis

5. RESULTS

The first 3 correlating sessions used the same mask on both frames, which was kept throughout the study in order to avoid differences in vector computing. The 4th session had a different mask, identical on both frames, placed in a similar way to the first sessions.

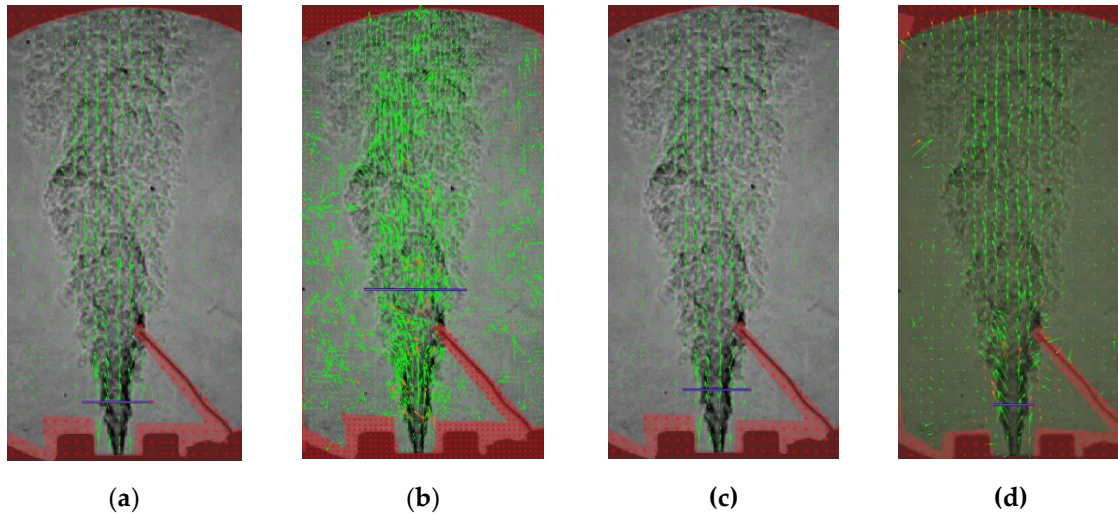


Fig. 4 Resulted vectors from the consecutive sessions: (a) session 1 – FFT 3 passes, (b) session 2 – FFT 3 passes, (c) session 3- FFT 2 passes, (d) session 4 – DCC 1 pass.

The results from the PIVlab analysis are interpreted in relation to the general theoretical evolution of axisymmetric hot RTJs. As SIV can only render line-averaged values, the generated U and V curves by PIVlab along a few inspection lines such as the purple ones which can be observed in Fig. 4, are used for data interpretation. As SIV can only render line-averaged values, the generated U and V curves by PIVlab along a few inspection lines such as the purple ones which can be observed in Fig. 4, are used for data interpretation. Fig. 5 depicts a very similar round, turbulent jet recorded by schlieren interferometry and its expected center line velocity map, resulted from the Jonassen and Settles investigation [12].

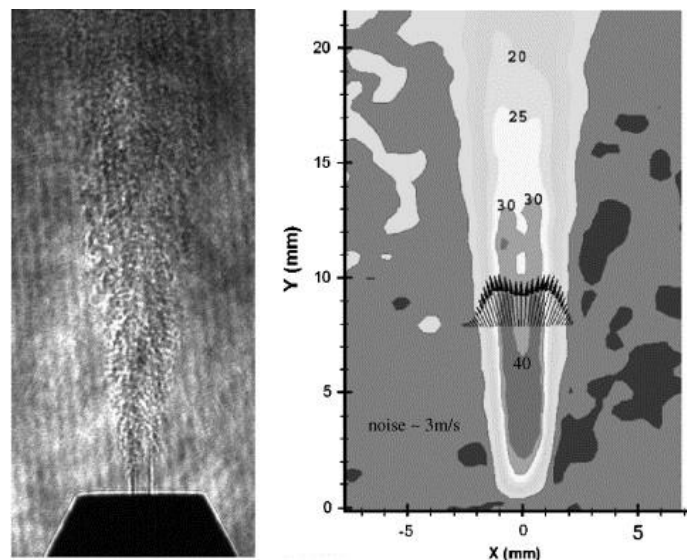


Fig. 5 Axisymmetrical helium RTJ in air [12].

The values obtained here will therefore not account for the center line velocity of the jet, as the one presented in Fig. 6, given the line-averaged character of the schlieren method, as determined by Schmidt [13] and explained in the Introduction section of this paper. In order to determine the jet's center plane velocity profile, an Inverse Abel Transform must be performed.

The first interrogation session performed 3 passes of different window sizes and steps, as specified in Table 2. It can be observed that the magnitude of the background vectors is too high to be eliminated by setting a velocity limit, as working with such a limit would also affect the vectors which can be found in the flow. As expected, due to the high speed at the exit of the RTJ, the resulted vectors closer to the thruster are of greater magnitude, denoting a higher velocity, while the jet's plumes are dispersing with less velocity at the superior limit of the jet.

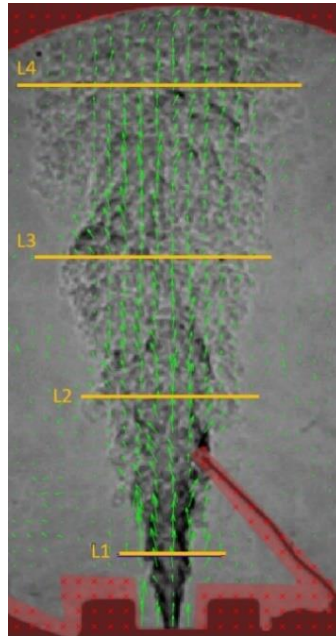


Fig. 6 Measurement lines across the RTJ.

The control lines from Fig. 6, are placed as follows: L1- 1mm, L2- 24mm, L3- 68mm, L4- 122mm.

The coordinate system used was the predefined system from PIVlab, where y increases towards the top, and x increases towards the right (determining U to be the lateral velocity and V the streamwise velocity), in relation with Fig. 6 and as displayed in Fig. 7).

The profile of the $V(y)$ velocity (in the y direction) along the control lines for session 1, should follow a gaussian distribution, evolving from a very low value found at the outer layer of the jet, to reach a peak when crossing the jet's centerline and afterwards descending to the other jet's limit. This is caused by the jet's dispersing mechanism, described by Fig. 7. The $U(x)$ velocity should present an anti-symmetric profile, with the displacement vectors following the axisymmetric character of the jet

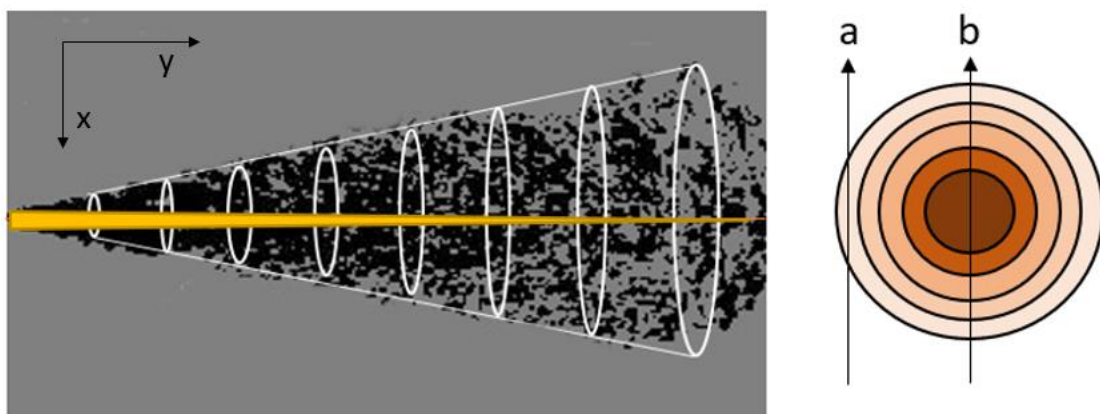
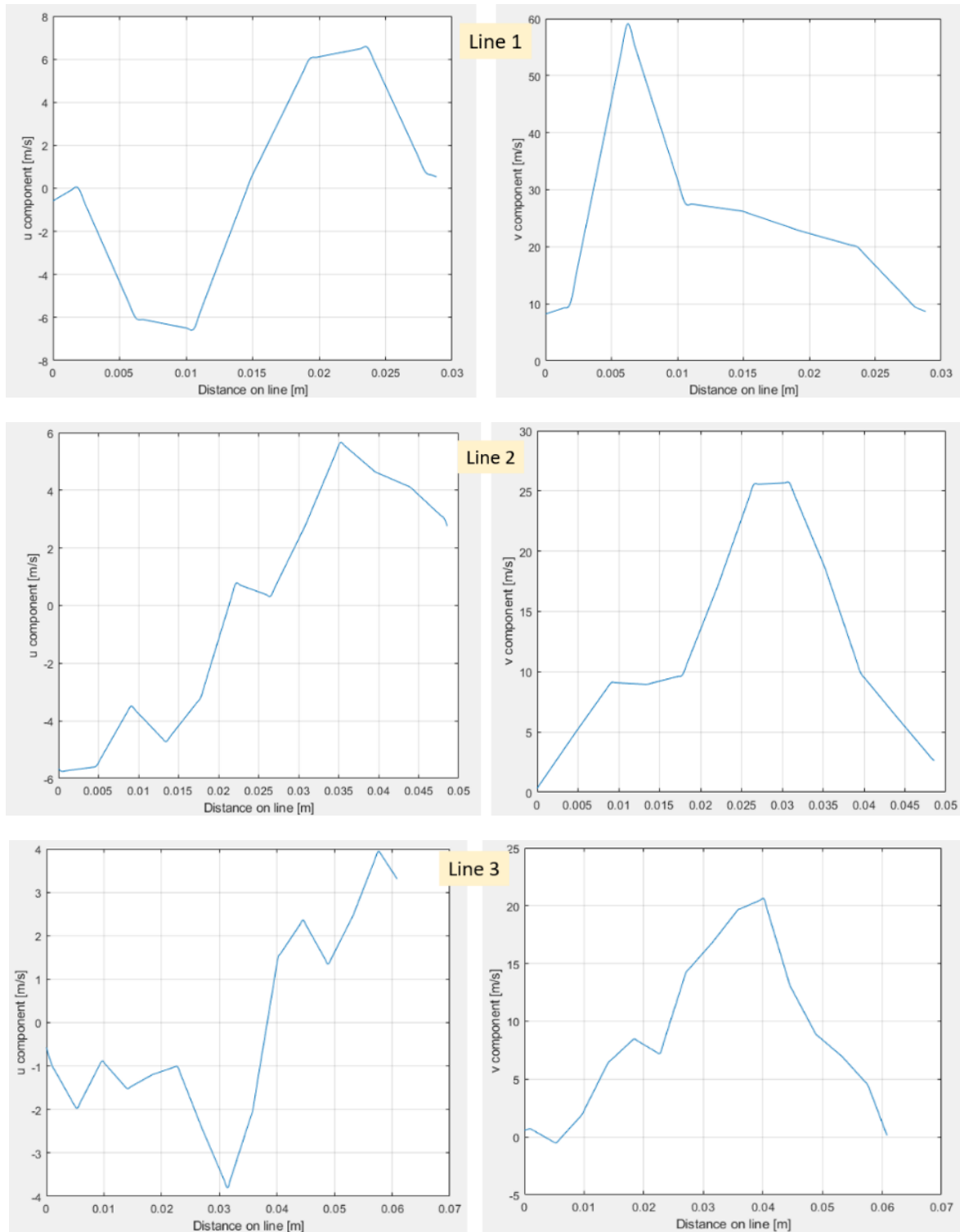


Fig. 7 RTJ's structure: (left) graphical representation of the theoretical centerline velocity profile and (right) the light crossing through the outer layer a, compared to the integrated path found in the center plane (b).

For all the post processing sessions, the y increases towards the top, while the x increases towards right. The images have been processed as in Fig. 4 , with the same coordinates as in Fig. 7, (left). Data was extracted on 4 lines that split the jet, in order to form a conclusion about the information offered per each jet section.



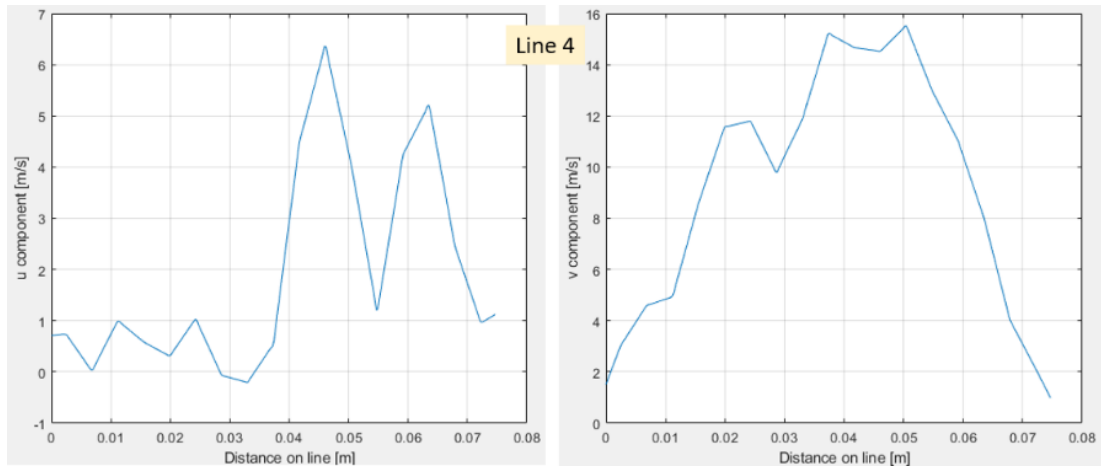
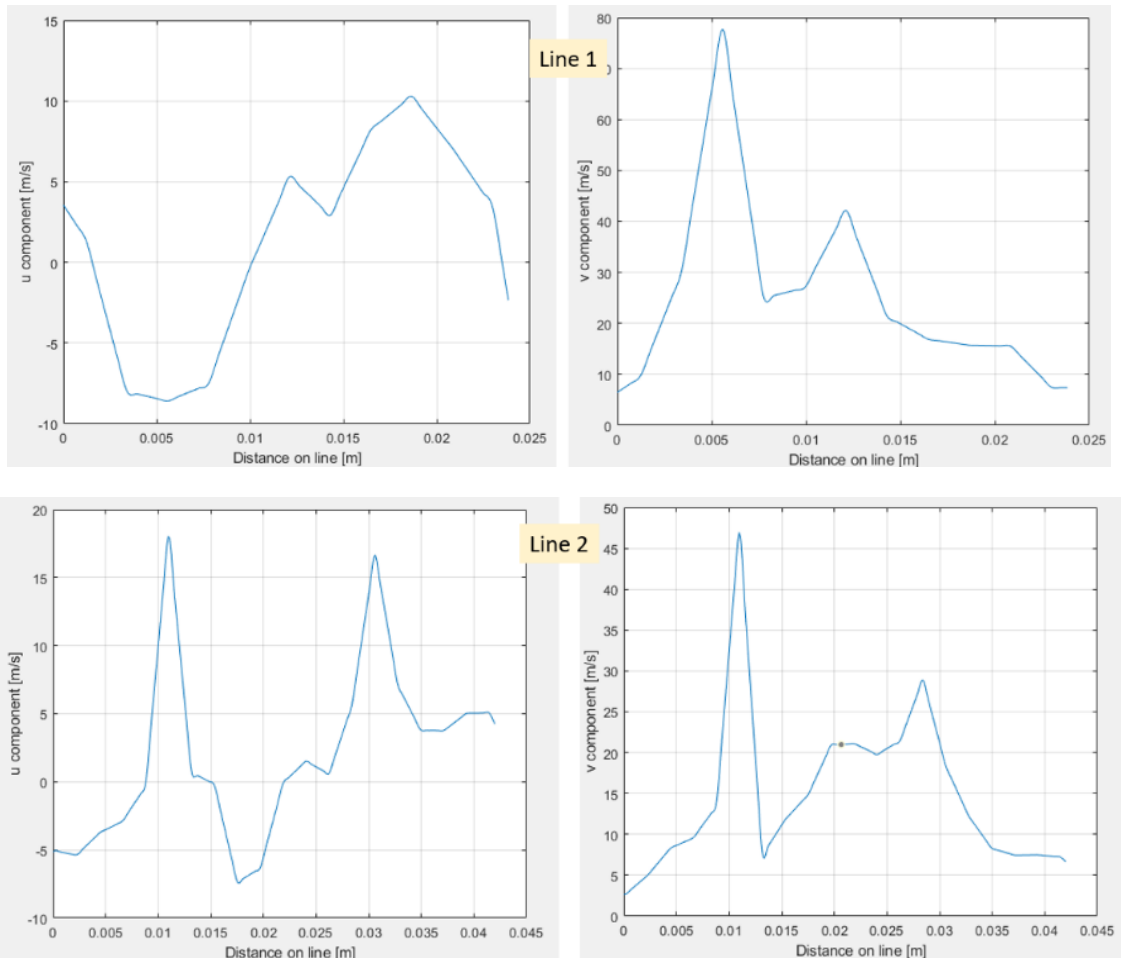


Fig. 8 U and V velocity profiles of the first session, along the integration lines.

The velocity maps obtained by cross-correlation provide a smaller magnitude of the velocities, when compared to the expected velocity values. The thruster was designed to expel the jet at a speed over 1000m/s, while the measurements, except for a few points present on the DCC map, present much lower values, which prove to be irrelevant for the velocity study.

Disregarding the values for the velocity, and focusing only on the shape of the graphs, it can be concluded that for the first session, the V profile closer to the ideal gaussian shape, can be found in Line 2, while the U velocity profile can be found for Line 1. However, all graphs present limited scattered data, and therefore fitting a progression curve for the vectors can be quite challenging. These results have not benefitted from the interpolation of missing values.



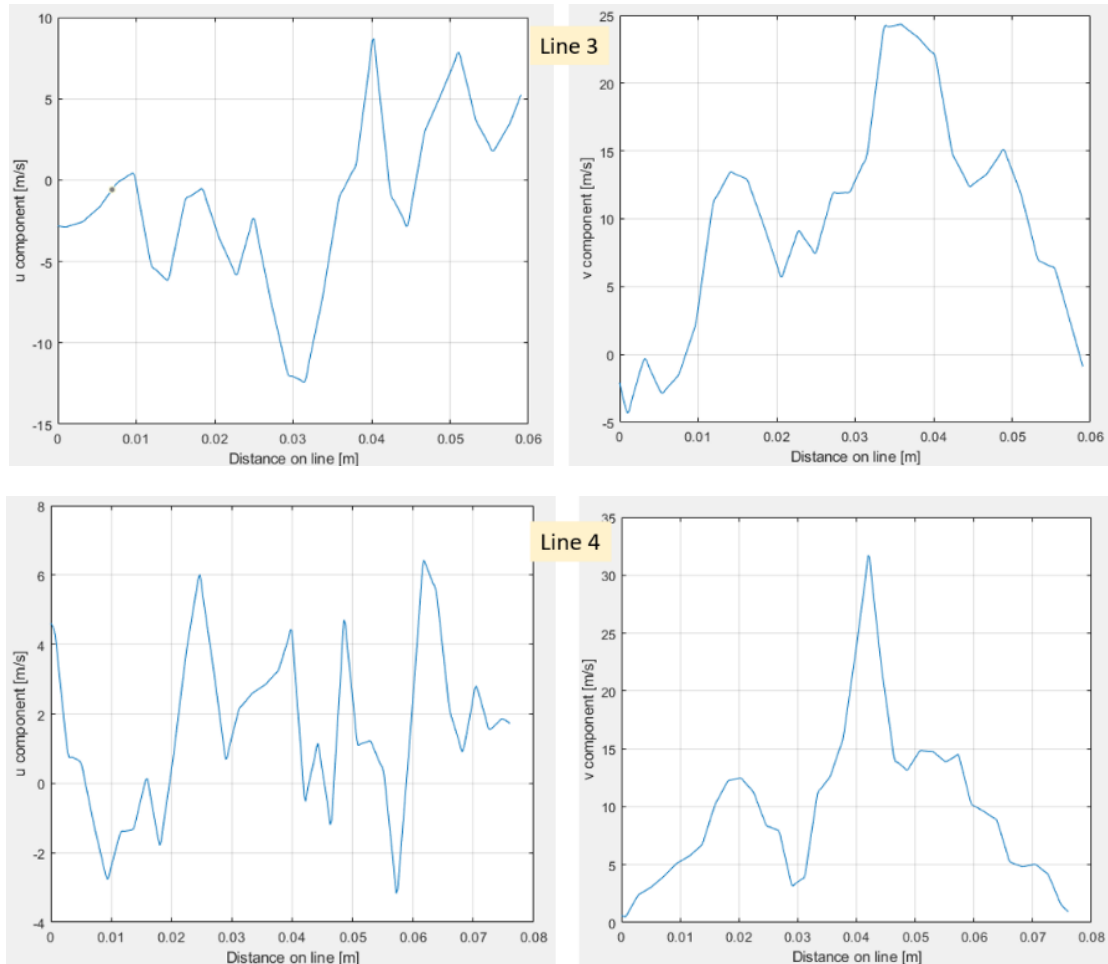
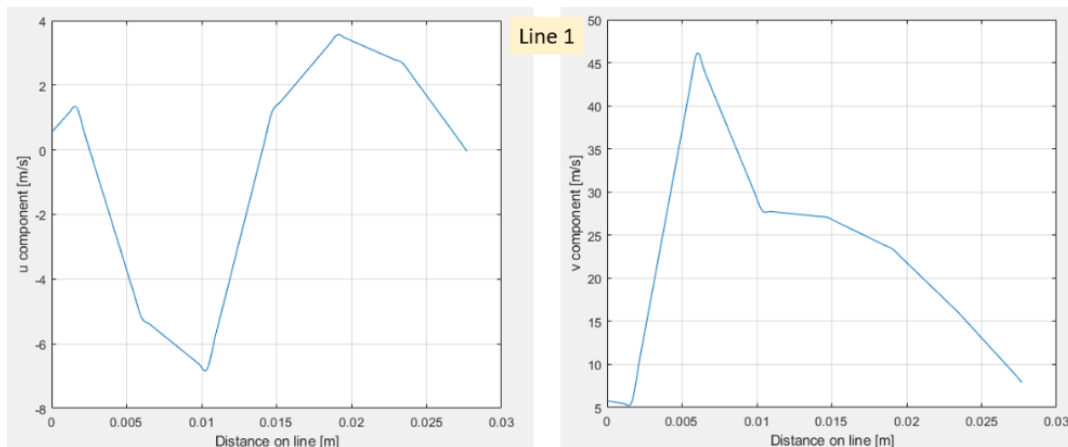


Fig. 9 U and V velocity profiles of the second session, along the integration lines.

The second post processing session, using 3 steps, but adding a smaller interrogation window of 8x4 pixels, presents an increase in the vector population. As specified before, if the data sample is larger, the results are more accurate. However, in this case, the jet reflects out of the vacuum chamber's casing, causing the appearance of stray elements in the background, that cannot be eliminated.

These elements are perceived as signals and result in false correlation values, and are also amplified with the vectors. This session benefitted from missing data interpolation, and the vectors generated by this can be observed as bright orange arrows, in Fig. 4, the third image from left to right. For this session, Line 1 presents the best U profile, while the best V peak can be found in Line 4, as depicted in Fig. 9.

The third session rendered good results on the first line for the U velocity, and on the 3rd line for the V velocity, as depicted by Fig. 10.



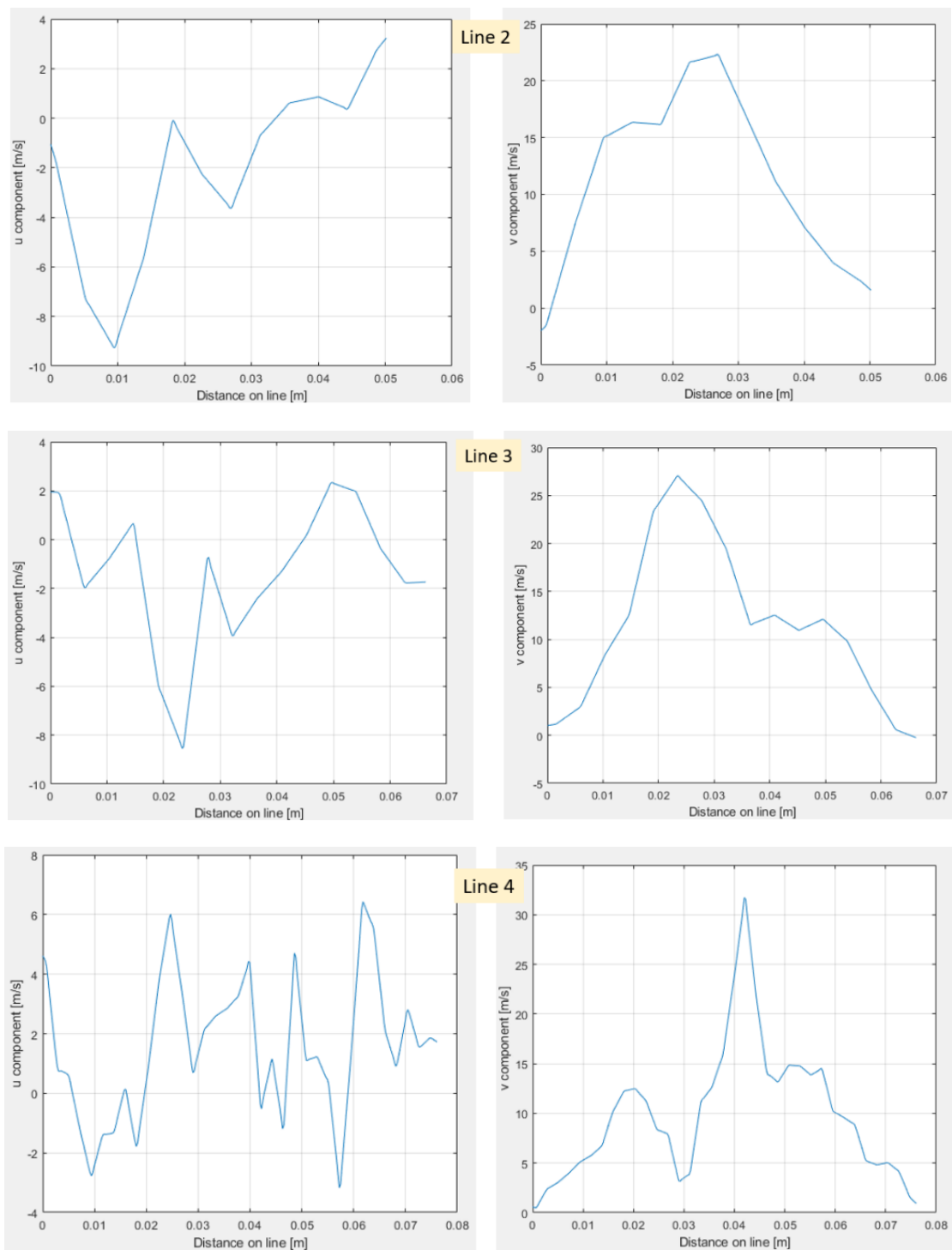


Fig. 10 U and V velocity profiles of the third session, along the integration lines.

Although the data sample has been smaller than that obtained by session 1 and session 2, the interrogation window and pass size were more appropriate, by looking at the 4th interrogation line. Here, the U velocity varies by another law, as the vorticities of the jet's plumes no longer vary similar to the ones at the jet's exit.

The DCC analysis was performed on a raw set of the schlieren images, as no color index was necessary to performed the measurement and it was observed that the image saturation does not play a role in the cross correlation of the images.

While the DCC performed very well in determining more accurate values of the flow velocities than the ones provided by the FFT cross-correlation, it presents the expected issue of data scarcity, as it only applies a singular pass, equal to the size of the image. The resulted velocity at the exit of the flow, calculated from the image, with the specifications provided in Table 1, were close to 900m/s. The thruster was designed to reach over Mach 3.5, but several sources of errors can be encountered in this measurement, such as the delay between frames, which can be enough for some sections of the jet where the flow is slowed down, but it could miss the turbulent elements propagating at high speed. Secondly, the line-averaged character of the schlieren technique, which impairs such measurements must be taken into account. These two sources of errors are also valid for the FFT cases.

6. CONCLUSIONS AND FUTURE WORK

The main conclusion of the present study is that while the velocity magnitude couldn't be determined within reasonable accuracy limits, a graphic profile description of the velocity profiles along 4 interrogation lines which horizontally section the jet, has been obtained.

The main reason behind the lack of accuracy in velocity magnitude measurements when performing SIV is caused by the path-integrated character of the schlieren images, which represent a projection of the integrated density field and can only be post processed to render line-averaged values of velocities.

Most papers, such as [1,5,6,12], find that SIV methods can provide a data accuracy between 20%-100%, depending on the type of the studied flow and the post processing method.

For the present test case, SIV was performed by analysing the axisymmetric jet through image cross-correlation. Four post processing sessions with different settings were performed. The first three sessions used an FFT approach, with different interrogation windows and steps.

It has been observed that the second session provided a larger sample interval, due to the dimension of the last step applied, which involved a smaller interrogation window and step. However, the resulted velocity map also contained an amplified number of spurious vectors, generated by the natural convection developing in the background. Reducing the interrogation area has a negative effect on the vectors generated at the outer extremities of the jet's shear layers. The shear layer's elements can be mistaken by the algorithm with elements resulted from the natural convection. This leads to false values of the correlation peaks, generates false vectors and increases the overall error of the measurement.

The first and third sessions rendered similar results, given the similar size of the smallest pass applied. They also present spurious vectors in the background, but at a smaller scale compared the ones found in the second session. An advantage of the larger interrogation windows used here is that the distinction between the vectors can be achieved easily. Nonetheless, for the images presented here, velocity limits cannot be imposed in order to totally eliminate the spurious vectors because it would also brush off real vectors, and therefore reduce the sample size. The sample size is given by the Central Limit Theorem which states that for a sample size to be relevant, it needs to account for 30-50 measurement points [26].

The DCC measurements computes the correlation matrix in the spatial domain. The DCC method's settings were adapted by considering the previous sessions' results. Therefore, an interrogation area of 16x8 was used, as this was proven to be the best compromise between having a relevant sample size and the spurious vectors impact. Providing data very close to the expected value of the jet's exit velocity, the DCC method has been proved to be unreliable given the data scarcity resulted from the method's character which only allows a single pass computation.

In order to improve the results of the method, there are two important aspects which can and must be improved.

The first aspect is providing better schlieren images, which can be achieved by providing a recording speed fitted to the turbulent element's development time. Another possibility is performing two separate sessions, the first one concentrated on the lower part of the jet, where the jet's density is higher, and recording images with a lower contrast, and a second recording session on the upper limit with a slightly higher contrast. This could reduce the level of the natural convection in the first recording session's case.

The second aspect to be taken into consideration is providing a theoretical profile of the flow's center plane velocities and compare it with a statistical method, such as the Abel Inverse Transform, to account for the 3D character of the flow.

Data gathered by physical instrumentation introduced in the flow, such as a hot-wire rake probe or even a comparison with data obtained from applying different visualization methods should be provided in order to better assess the error and accuracy of the SIV method.

ACKNOWLEDGEMENT

This work was carried out through the “Nucleu” Program, within the frame work of the National Plan for Research, Development and Innovation 2023-2026, supported by the Romanian Ministry of Research, Innovation and Development.

REFERENCES

- [1] Morales, R.; 2018; Lagrangian schlieren image velocimetry measurements in exhaust plumes; Masters Theses; New Mexico Institute of Mining and Technology; Socorro, New Mexico;
- [2] Belmouss, M.; 2015; Effect of electrode geometry on high energy spark discharges; Master’s thesis; Purdue University; West Lafayette;
- [3] Arnaud, E.; Mémin, E.; Sosa,R.; Artana,G.; 2006; Schlieren image velocimetry applied to ehd flow; in Proceedings of the European Conference on Computer Vision, ECC;
- [4] Scarano, F.; 2008; Overview of PIV in supersonic flows; in *Particle Image Velocimetry*, Berlin, Heidelberg: Springer Nature, pp. 445-463;
- [5] Biswas, S.; 2018; Chapter 3- Schlieren image velocimetry (SIV); in *Physics of turbulent jet ignition*, Cham, Springer Nature; pp. 35-62;
- [6] Wu,Y.; 2001; Detection of velocity distribution of a flow field using sequences of Schlieren images; *Optical Lasers Engineering*; vol. 40(8);
- [7] Raffel, M. *et al.*; 2000; Background oriented stereoscopic schlieren for full-scale helicopter vortex, in 9th International Symposium on Flow Visualization, Heriot-Watt University; Edinburgh;
- [8] Scarano, F. *et al.*; 1999; Pattern recognition analysis of the turbulent flow; *Physics in Fluids*; vol. 11, no. 12; pp. 3808-3818;
- [9] Elsinga, G. *et al.*; 2003; Assessment and application of quantitative schlieren methods: calibrated; *Experiments in Fluids*; vol. 36, no. 2, pp. 309-325;
- [10] Elsinga, G. *et al.*; 2003; Assessment and application of quantitative schlieren methods with,” in Proceedings of PSFVIP-4; Chamoix;
- [11] Kindler, A. *et al.*; 2007; Recent developments in background oriented Schlieren methods for rotor; *Experiments in Fluids*; vol. 43; no. 2-3; pp. 233-240,.
- [12] Jonassen, M.; Settles, G.S. *et al.*; 2006; Schlieren “PIV” for turbulent flows; *Optical Lasers Engineering*; vol. 44; no. 3-4; pp. 190-207;
- [13] Schmidt, J. *et al.*; 2020; Seedless Velocimetry in a Turbulent Jet using Schlieren Imaging and a Wavelet-based Optical Flow Method; in *AIAA Scitech 2020 Forum*;
- [14] Eckstein, P. *et al.*; 2009; Digital Particle Image Velocimetry (DPIV) robust phase correlation; *Measurements in Science Technology*; vol. 20; no. 5;
- [15] Thielicke,W and Sonntag, R.; 2021; Particle Image Velocimetry for MATLAB: Accuracy and enhanced algorithms in PIVlab; *Journal of Open Research Software*; vol. 9(1); p.12,.
- [16] Nicoară, R. *et al.*; 2021; Experimental testing of small H₂/O₂ thrusters in atmospheric and vacuum 412 conditions; in Proceedings of the 7th Edition of the Space Propulsion Conference; online;
- [17] Settles,G.; 2001; Schlieren and Shadowgraph Techniques, Berlin, Heidleberg: Springer;
- [18] Meynart,R.;1983; Mesure de champs de vitesse d' ecoulements fluides par analyse de suites d' images; Universite Libre de Bruxelles;
- [19] Adrian, R.; 1991; Particle imaging techniques for experimental fluid mechanics; *Annual Review of Fluids*; vol. 23; pp. 261-304;
- [20] Westerweel, J.; 1993; Digital particle image velocimetry - Theory and Application; Phd Thesis; Delft Univeristy Press; Delft;
- [21] Willert, C.G.;1991;Digital particle image velocimetry, *Experiments in Fluids*; vol. 10; pp. 181-193;
- [22] Keane, R. *et al.*; 1992; Theory of cross-correlation analysis of PIV images; *Applied Scientific Research*; vol. 49; pp. 191-215;
- [23] Raffel,M *et al.*; 1998; Particle Image Velocimetry, A Practical Guide, Berlin, Heidelberg: ©Springer-Verlag;
- [24] Bastiaans, M. *et al.*; 1993; Cross-correlation PIV : theory, implementation and accuracy; EUT reports; Vol. 99; Technische Universiteit of Eindhoven;
- [25] Press,W.H.; Vetterling, W.T.; Teukolsky, S.A.; Flannerly, B.P.; 1992; Numerical Receipts- The Art of Scientific Computing; Third Edition; Cambridge University Press, Cambridge; Chapter 16;

[26] [Online]. Available: https://www.investopedia.com/terms/c/central_limit_theorem.asp. Accessed 26th of April 2023].

Disclaimer/Publisher's Note: The statements, opinions and data contained in all publications are solely those of the individual author(s) and contributor(s) and not of COMOTI or the editor(s). COMOTI and/or the editor(s) disclaim responsibility for any injury to people or property resulting from any ideas, methods, instructions or products referred to in the content.

DEVELOPMENT OF A STRATEGIC MANAGEMENT PERFORMANCE METRIC FOR PROJECTS FINANCIAL MONITORING

Maria-Cristina ARVINTE¹

„When you can measure what you are speaking about, and express it in numbers, you know something about it; but when you cannot measure it, when you cannot express it in numbers, your knowledge is of a meagre and unsatisfactory kind...”

William Thompson (Lord Kelvin)

Received: 17.05.2023
Accepted: 16.06.2023
Published: 14.07.2023

Copyright: The article is an Open Access article and it is distributed under the terms and conditions Creative Commons Attribution (CC BY) license (<https://creativecommons.org/licenses/by/4.0/>).



ABSTRACT: The purpose of this study is to identify a metric to assess the financial monitoring of a project financed from Romanian budget state using Balanced Scorecard. The assessment of the monitoring process will be implemented on 34SOL/2021 project, title: „Development and implementation of a modern solution to replace Romanian Naval Forces Fast Patrol Boats (Missile) propulsion systems”, acronym NAVYPROM, having the implementing duration of 24 months (1st of October 2021-30th of September 2023). This project was chosen to develop a Balanced Scorecard in order to assess the financial monitoring due to the large amount of financial data, a great number of human resources used and the multiple verifications foreseen in the procedure of the contracting authority, namely the Executive Unit for Financing of Higher Education, Research, Development and Innovation (UEFISCDI). There was designed a contract map with clear established objectives, measurements and targets. The computed Balanced Scorecard on established periods shows a proper direction of contract management meaning a good project monitoring.

KEYWORDS: Balanced Scorecard, financial management, financial reporting, performance, continuous improvement

1. INTRODUCTION

Projects that imply a lot of human and material resources need to be financial monitored in an accurate way and to achieve continuous improvement during the implementation phase. Moreover, research projects like 34SOL/2021, financed by UEFISCDI, from budget state, have a lot of financial constraints imposed through contract. This study identifies a method to measure the efficiency of financial monitoring process that will show if the project converges in a good direction. The method consists in developing a Balanced Scorecard based on contract and resources needed. Balanced Scorecard is a representative metric of strategic management

¹ Romanian Research and Development Institute for Gas Turbines COMOTI

performance. It is developed having the starting point the strategy of a company. This metric will show the positive or negative direction for that organisation.

The most common tools for financial assessment are Key Performance Indicators (KPIs) and Balanced Scorecard. KPIs are a set of independent indicators that don't reflect any correlation between them. Balanced Scorecard has the advantage that is a composed indicator that offers the information if the project is on a good track or on a neutral track and some measures need to be done in order to improve the situation or on a bad track that requires serious and urgently measures to be taken. The implementation of both approaches was studied during an internship in the Planning Department of Hungarian Central Statistical Office (HCSO), in 2008. Balanced Scorecard was designed in the frame of the strategy and an IT application was ensured in order to calculate the indicator. The strategy for the period 2005-2008 ([1]) was structured respecting the project management principals and one of its objectives was to implement tools as Balanced Scorecard. In the present study, the Balanced Scorecard will be developed for 34SOL/2021 research project that is implemented by COMOTI Romanian Research and Development Institute for Gas Turbines (COMOTI) as coordinator and has not only a huge budget, but also a very ambitious scope, reflected by the title of project, namely „*Development and implementation of a modern solution to replace Romanian Naval Forces Fast Patrol Boats (Missile) propulsion systems*”. The current geopolitical situation adds much importance to the project scope and relays on the successful finalised project 4SOL/2017, that smooth the path for the biggest technological transfer in Romania, implemented by COMOTI.

The risk in any research activity was not taken into account in the present study due to the fact that research contracts financed from budget state have clear provisions regarding the above-mentioned risk. UEFISCDI assumes this risk together with the contractor. In the overall system of established measurements for Balanced Scorecard there are several that can be indirectly linked to this risk, mostly the ones for the perspective Employee Learning and Growth.

2. 34SOL/2021 A CHALLENGE FOR FINANCIAL MONITORING PROCESS

34SOL/2021 has a budget of 10 million lei (over 2 million in Euro), financed from state budget and around 800 thousand lei co-financing (over 150 thousand in Euro). The consortium, led by COMOTI, encompasses six different organisations: two national research institutes, three universities and one enterprise, from private sector, all spread among all macro regions of Romania, at NUTS 1 level according to Regulation (EC) No 176/2008 of the European Parliament and of the Council of 20 February 2008. Figure 1 captures some impressive numbers related to 34SOL/2021 ([2]).

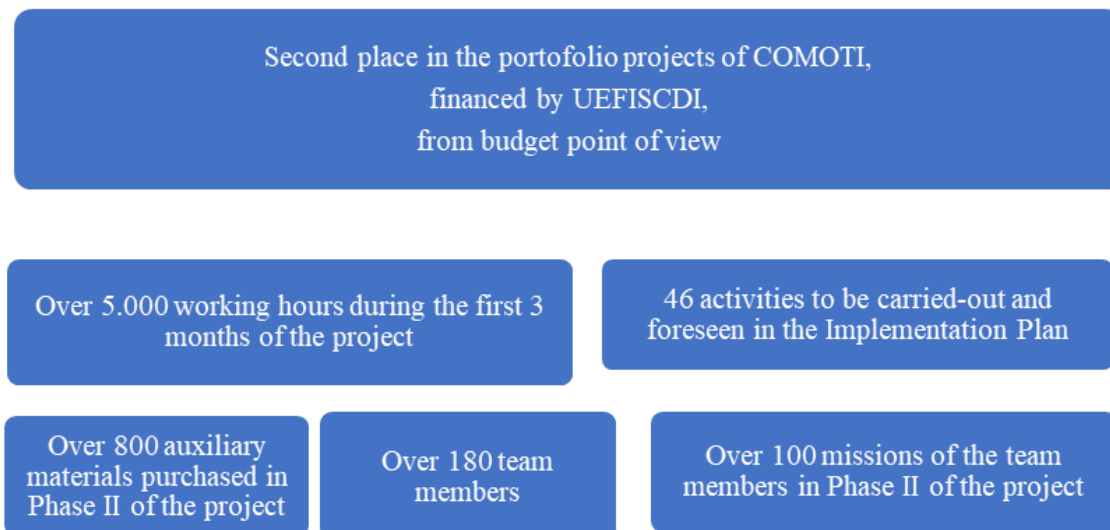


Fig. 1 34SOL/2021 in figures

3. PREMISES FOR DEVELOPING CONTRACT MAP, SETTING OBJECTIVES AROUND THE FOUR PERSPECTIVES AND BUILDING MEASUREMENTS

Balanced Scorecard, developed by Robert Kaplan and David Norton, was presented in Harvard Business Review in 1992 and it can be described as “a carefully selected set of quantifiable measures derived from an organisation’s strategy” ([3]), as Paul R. Niven writes in his book “Balanced Scorecard Step-by-step: Maximizing Performance and Maintaining Results” ([4]). It is currently used by over 70% of the Fortune 1.000 companies in U.S.A. to manage performance at every level of the company. This tool of strategic management groups and quantifies strategy at different organizational levels, enabling the assessment performance and improvement of internal processes.

When developing a Balanced Scorecard around the organisation strategy, there are four perspectives: Customer, Internal Processes, Employee Learning and Growth and Financial. The Balanced Scorecard developed for 34SOL/2021 financial monitoring assessment uses the contract between COMOTI and UEFISCDI. The contract will serve as strategy for developing the Balanced Scorecard. First step is to map the contract meaning objectives identification. Figure 2 illustrates the phases for developing Balanced Scorecard, adapted to 34SOL/2021 contract after Matt Evans, trainer on Balanced Scorecard, presented on its online courses ([5]).



Fig. 2 Steps in the process of building a Balanced Scorecard for 34SOL/2021 project

When defining the strategic objectives around the four perspectives, there are envisaged the four questions, presented in the figure below, after Matt Evans presented on its online courses ([5]), adapted to 34SOL/2021 contract.

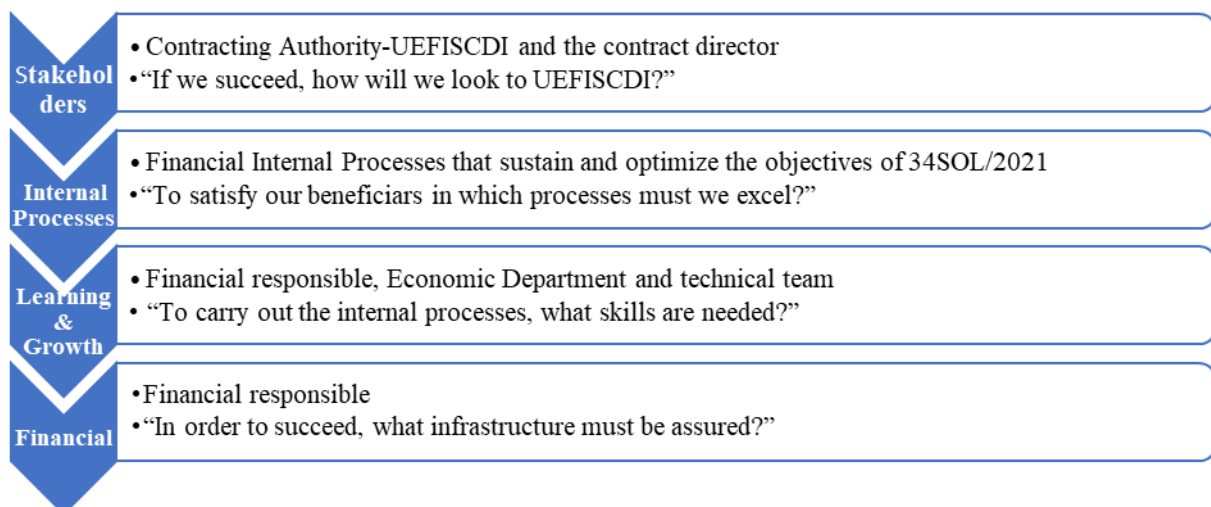


Fig. 3 The four perspectives of strategy objectives of Balanced Scorecard

When the objectives were developed, the following principals governed the process, presented by Matt Evans on its online courses ([5]): relevant, specific, simple, attainable and ownership, while the measurements had the following characteristics: useful, measurable, actionable and balanced.

Once that the objectives were set, the next steps, described by Matt Evans, trainer on Balanced Scorecard, presented on its online courses ([5]), in order to obtain a Balanced Scorecard is presented below and detailed in Table 1 of chapter 4 of this article on 34SOL/2021 Contract.



Fig. 4 Phases in developing Balanced Scorecard

4. CONTRACT MAP FOR BALANCED SCORECARD DEVELOPING

The designed contract map takes into consideration the performance dimension of Balanced Scorecard. The objectives set on the four perspectives: financial, customer, internal processes and learning, reflect the continuous improvement on long term, even after finalising the contract. Being in the last phase of 34SOL/2021 project implementation, it allowed to observe processes errors and correct. For example, one is the assessment of partners who have no experience in managing such projects and from financial point of view, financial reporting to UEFISCDI for such partners, implies a lot of assistance.

Figure 5 represents the Contract Map for 34SOL/2021 around the four perspectives, adapted from examples given by Robert S. Kaplan and David P. Norton in their book „*The Strategy-Focused Organization*” ([6]). The objectives were established according to the restrictions imposed by contract and strategy of COMOTI. The objectives set on the financial perspective take into consideration the cost-efficiency and value for money. On the customer perspective, the objectives are set with regard to COMOTI’s partnerships, on one hand and with UEFISCDI and on the other hand with all project partners. The objectives set on internal processes are focusing on the efficiency of financial monitoring of the project and financial and accounting procedures in COMOTI.

Financial	Create Value-Added	Endowment of Research Departments Involved in Gas Turbine Naval Applications	Reduce Budget Variance	Increase Timeliness and Punctuality of Payments
Customer	Maximize Timeliness of answers to requests of point of contact of UEFISCDI	Strong Dissemination of the Project Results	Strengthening Partnerships	Assessment and Increase Support to Partners
Internal Processes	Facilitate Cost Management	Reduce Financial Reporting Error	Decrease Invoice Cycle Time	Maximize Timeliness of Cash Flow Reporting
		Implement Best Practices		
Learning	High Skill Levels	Optimum Average Years of Experience	Increase Internal Communication Rating	Cross Functional Teams

Fig. 5 34SOL/2021 Contract Map for designing the Balanced Scorecard

Table 1 reflects the measurements for Balanced Scorecard according to 34SOL/2021 Contract Map and presented in the standardised manner as in the examples given by Robert S. Kaplan and David P. Norton in their book *“The Balanced Scorecard Translating Strategy into Action”* ([7]) and Robert S. Kaplan and David P. Norton in their book *„The Strategy-Focused Organization. How Balanced Scorecard Companies Thrive in the New Business Environment”* ([6]). For every objective were identified measures that have a serious impact over the project and the following principles represented the foundation:

- **Minimizing the ineligible costs;**

Although it is desired to not have any ineligible costs, there is the subjective interpretation of Contracting Authority in this matter. This is the reason for including a measure with a high weight in the overall system (*“Percentage of ineligible costs of the allocated budget”*) of measurements created and detailed in Table 1.

- **Endowment of Research Departments in order to assure the successful implementation of the project;**

It was necessary to ensure IT tools, both software and hardware for the technical staff that allow to organise meetings at partners premises and to present to the beneficiary of the results of the project working documents. Assets bought under the value of 2.500 lei were used mainly in micro production unit.

- **Minimizing the deviation of the planned costs versus actual costs;**

The measurements *“Percentage of the amount spend supplementary”, “Percentage of reallocation of amount planned for each category of costs: direct personnel costs”, “Percentage of reallocation of amount planned for each category of costs: logistics”, “Percentage of reallocation of amount planned for each category of costs: delegations”, “Percentage of reallocation of amount planned for each category of costs: indirect costs”* and *“Percentage of overall reallocation”* were designed in order to quantify the deviations from the planned budget and possible loops in the research activities that consumes unpredicted budget.

- **Establishing long-term partnerships both with UEFISCDI and partners involved;**

Nowadays, in order to benefit from grants, establishing partnerships is crucial. Also, strengthening the communication with the contact point with UEFISCDI and deliver punctual, accurate and timely answers contribute to a good image of COMOTI. Objectives in this area were set in order to assign the proper importance to this action.

Objectives like *“Maximize Timeliness of answers to requests of point of contact of UEFISCDI”, “Assessment and Increase Support to Partners”, “Strengthening Partnerships”* is considered a trigger in the technical and financial reporting. Knowing the partners very well and their experience reduces the risk of encountering a large type of errors.

- **Optimizing the financial and monitoring processes related to 34SOL/2021 contract;**

The objectives identified for the Internal Process perspective are focusing on the financial monitoring of the project carried out in the Planning and Accounting Departments in order to ensure a sound financial reporting. The dynamic of costs registered and planned on short term impose a financial reporting with high frequency to the technical responsible. It was commonly agreed between the technical team and financial team that at every two weeks, a situation with the encountered costs and the sum available for spending to be transmitted. This is the reason for including the measure *“Number of reports with all registered costs and balances send to technical responsible”* with an important weight assigned. The measurement *“Number of reports with personnel costs send to technical responsible”* is important because the technical responsible approves the number of hours in the monthly timesheets for the staff working on the project. Both measures are designed for a proper decision making. Including the measure *“Number of times of confrontation between financial responsible evidence and registrations in accounting system”* is an important tool for identifying

errors in primary accounting documents in terms of registration in the accounting system of COMOTI and in UEFISCDI platform for the financial monitoring. The registration in the accounting system of COMOTI and in UEFISCDI platform are made by different persons in COMOTI with different skills. Both measures are considered a helpful tool in the financial reporting in an accurate manner. “Average time of invoice cycle time” measure was included because it reflects the efficiency of processing bills for payment and can directly impact the project as is stated in the article “*Invoice Cycle Time: What Is It and How to Improve It*” from <https://planergy.com> ([8]). The cycle of an invoice starts with its entering in COMOTI, it passes on different departments in order to ensure all the conditions foreseen in the Romania laws and the final step is the payment phase. The longer is this cycle in every organisation, the more money are spent. So, to decrease the above mention cycle is considered important. If the invoice or other documents (like contracts) don't specify a certain deadline for paying, the Romanian law considers 30 days the term for payment of the invoice.

- **Solid dissemination of the project results;**

In 2022, UEFISCDI accentuated the dissemination of the results encountered. It is expected to follow the European Commission politics to maximize the dissemination of the results. In Table 1 were included the two measures for every type of result requested by UEFISCDI.

- **Very good internal communication;**

The internal communication between teams with different background it turned out to be a major factor in the decision-making process.

- **High frequency of financial reports sent to the technical responsible;**

- **Continuous improvement assured;**

The objective “*Maximize Timeliness of Cash Flow Reporting*” takes into consideration the number of corrections presented in the financial situations. The Economic Department requests regularly the financial situation of the project in order to ensure a smooth process of the organisation's liquidity, flexibility and overall financial performance. Minimizing the errors in this reports are very important.

In order to ensure the continuous improvement, there were included the measures: “*Percentage of number of errors corrected regarding the financial monitoring process compared to the previous phase*” and “*Number of errors corrected regarding the accounting primary documents compared to the previous phase*” under the objective “*Implement Best Practices*”.

- **High-skilled human resources involved.**

For every objective were set one or more measurements. The periods for collecting the data were split as follows:

- 1st October-31st December 2021;
- 1st January-30th June 2022;
- 1st July-31st December 2022;
- 1st January-30th June 2023 (with estimated data).

For each period there were calculated values for each measurement established. For the calculated values were established ranges for the three categories: red, yellow and green. If the value of an indicator for a period is on red it means that the financial management is not suitable and serious measures need to be implemented in order to correct the situation, yellow a neutral state meaning that the financial management is nor good, nor bad, while green signifies a good path and a good financial management implemented. For each measure calculated was assigned a weight due to the fact that all objectives don't have the same impact on the financial management and don't contribute equally in the final value of Balanced Scorecard. There were established 17 objectives around the four perspectives of Balanced Scorecard. Strategic management implies continuous improvement and that is the reason for including in table 1 initiatives for each measure.

Table 1. Balanced Scorecard – Strategic Objectives, Measurements, Targets and Initiatives

Strategic Objectives	Measurements	Range of values for 3 situations: red-bad, yellow-neutral, green-good			Weight	Initiatives for continuous improvement
<i>Create Value-Added</i>	<i>Percentage of ineligible costs of the allocated budget</i>	> 1%	0,5%-1%	0%-0,25%	5%	a) Permanent communication between technical responsible and financial responsible; b) Financial responsible designated for financial monitoring; c) Financial monitoring by department's economists for research department's involved;
	<i>Percentage of the amount spend supplementary</i>	> 10%	7%-10%	0%-7%	5%	a) Financial reporting on the costs registered to technical responsible every two weeks.
<i>Endowment of Research Departments Involved in Gas Turbine Naval Applications</i>	<i>Percentage of actual purchased equipment comparing to planned situation</i>	<80%	80%-90%	>90%	3%	a) Purchase a major part of planned equipment in the design phase.
	<i>Percentage of assets less than 2.500 lei (without VAT) from overall assets purchased financed by UEFISCDI</i>	<25%	25%-50%	>50%	3%	a) Purchase assets less than 2.500 lei (without VAT) in order to smooth the activities related to contract scope.
<i>Reduce Budget Variance</i>	<i>Percentage of reallocation of amount planned for each category of costs: direct personnel costs</i>	>30%	15%-30%	<15%	1%	a) Financial reporting on the costs registered to technical responsible every two weeks.
	<i>Percentage of reallocation of amount planned for each category of costs: logistics</i>	>30%	15%-30%	<15%	1%	a) Financial reporting on the costs registered to technical responsible every two weeks. b) Financial reporting on the planned acquisitions to the technical responsible at every quarter.
	<i>Percentage of reallocation of amount planned for each category of costs: delegations</i>	>30%	15%-30%	<15%	1%	a) Financial reporting on the costs registered to technical responsible every two weeks.
	<i>Percentage of reallocation of amount planned for each category of costs: indirect costs</i>	>30%	15%-30%	<15%	1%	a) Financial reporting on the costs registered to technical responsible every two weeks.
	<i>Percentage of overall reallocation</i>	>30%	15%-30%	<15%	4%	a) Financial reporting on the costs registered to technical responsible every two weeks.
	<i>Percentage of overall reallocation</i>	>30%	15%-30%	<15%	4%	a) Financial reporting on the costs registered to technical responsible every two weeks.
<i>Increase Timeliness and Punctuality of Payments</i>	<i>Percentage of overdue payment for logistics invoices from payment deadline</i>	70%>	30%-70%	<30%	4%	a) Check the status of payment for logistics invoices on a weekly base and prepare the situation with unpaid invoices weekly for the payment responsible and Economic Director. b) Solved every issue requested by Purchasing Department and researchers responsible for the

Strategic Objectives	Measurements	Range of values for 3 situations: red-bad, yellow-neutral, green-good			Weight	Initiatives for continuous improvement
						economic order.
	<i>Exceeding deadline of payments from 34SOL contract by COMOTI to partners</i>	> 8 days	5-8 days	0-5 days	2%	a) Monitoring the inputs in the treasury account of COMOTI on daily bases. b) Preparing all the necessary documents in a timely manner for the payment responsible. c) Inform the partners about payment in order to prevent any disparity in the process.
<i>Maximize Timeliness of answers to requests of point of contact of UEFISCDI</i>	<i>Percentage of exceeding the deadlines of the point of contact of UEFISCDI from total requests</i>	>5%	0%-5%	0%	5%	a) Implement efficient time management.
<i>Strong Dissemination of the Project Results</i>	<i>Number of articles, presentations at conferences, chapters in scientific books, published studies, number of patents</i>	0-3	3-5	>5	4%	a) Offering assistance to all partners with scientific background in order to maximize the dissemination dimension.
	<i>Regular update of COMOTI web-site dedicated to 34SOL</i>	Less than yearly	Yearly	Semestrial	4%	a) Name one responsible for updating the web-site.
<i>Strengthening Partnerships</i>	<i>Number of meetings with partners per contract phase</i>	0	1	2	2%	a) Organise meetings with partners whenever are problems encountered.
	<i>Number of missed requests from partners</i>	> 5	3 - 5	< 3	2%	a) Implement efficient time management.
<i>Assessment and Increase Support to Partners</i>	<i>Assessment of partners experience in projects with budget state financing</i>	NO	NO	YES	4%	a) Develop a check-list for the assessment of partners regarding their experience in project management contracts with budget state finance.
	<i>Support in the financial reports for the partners with no experience in projects with budget state finance</i>	NO	NO	YES	4%	a) Checking all the accounting primary documents and carry out the financial report.
<i>Facilitate Cost Management</i>	<i>Number of reports with all registered costs and balances send to technical responsible (financial report carried out at every two weeks and send to the technical responsible)</i>	< 6	6 - 12	> 11	5%	a) Present all the financial reports to the technical responsible; b) Communicate with accounting unit and all economists from research departments.
	<i>Number of reports with personnel costs send to technical responsible</i>	< 3	3 - 5	> 5	5%	a) Present all the financial reports to the technical responsible; b) Communicate with

Development of a strategic management performance metric for projects financial monitoring

Strategic Objectives	Measurements	Range of values for 3 situations: red-bad, yellow-neutral, green-good			Weight	Initiatives for continuous improvement
		Red	Yellow	Green		
						accounting unit and all economists from research departments.
<i>Reduce Financial Reporting Error</i>	<i>Number of times of confrontation between financial responsible evidence and registrations in accounting system</i>	<i>< 5 times</i>	<i>5-10 times</i>	<i>> 10 times</i>	5%	a) Financial situation carried out and send to the technical responsible every two weeks.
<i>Decrease Invoice Cycle Time</i>	<i>Average time of invoice cycle time</i>	<i>>60 days</i>	<i>30 - 60 days</i>	<i>< 30 days</i>	3%	a) Monitoring the accounting registrations. b) Collect copies of all primary documents. c) Collaborate with the accounting unit in order to correct all errors.
<i>Maximize Timeliness of Cash Flow Reporting</i>	<i>Number of corrections presented in the financial situations for ensuring the payments for all categories of costs</i>	<i>> 10</i>	<i>5 - 10</i>	<i>0 - 5</i>	3%	a) Monitoring the accounting registrations. b) Collect copies of all primary documents. c) Collaborate with the accounting unit in order to correct all errors.
<i>Implement Best Practices</i>	<i>Percentage of number of errors corrected regarding the financial monitoring process compared to the previous phase</i>	<i>3% <</i>	<i>3% - 5%</i>	<i>>5%</i>	3%	a) Communicate with accounting unit and all economists from research departments.
	<i>Number of errors corrected regarding the accounting primary documents compared to the previous phase</i>	<i>10 <</i>	<i>10-15</i>	<i>> 15</i>	3%	a) Communicate with accounting unit and all economists from research departments.
<i>High Skill Levels</i>	<i>Percentage of personnel with experience on similar projects</i>	<i>60% <</i>	<i>60%- 85%</i>	<i>>85%</i>	5%	a) Maintaining the financial and other advantages offered by COMOTI for PHD researchers according to intern regulations.
	<i>Percentage of 34SOL/2021 management with PHD</i>	<i>25% <</i>	<i>25%- 40%</i>	<i>>40%</i>	2%	a) Maintaining the financial and other advantages offered by COMOTI for PHD researchers according to intern regulations.
	<i>Percentage of management with PHD candidate</i>	<i>10% <</i>	<i>10%- 15%</i>	<i>>15%</i>	2%	a) Involvement of young researchers in the project; b) Know-how transfer from experienced researcher to young researchers.
<i>Optimum Average Years of Experience</i>	<i>Percentage of executive staff with optimum number of experience years (5 years-15 years) in the Economic Department</i>	<i>< 40%</i>	<i>40% - 65%</i>	<i>>65%</i>	3%	a) Maintaining the financial and other advantages offered by COMOTI for employees.

Strategic Objectives	Measurements	Range of values for 3 situations: red-bad, yellow-neutral, green-good			Weight	Initiatives for continuous improvement
		3<	3-5	>5		
<i>Increase Internal Communication Rating</i>	<i>Number of e-mail messages and presentations regarding the rules of contract to the technical staff</i>	3<	3-5	>5	3%	a) Maintaining the financial and other advantages offered by COMOTI for employees.
<i>Cross Functional Teams</i>	<i>Number of staff with different specialisations in the Economic Department (project management, accounting, controlling, auditing)</i>	< 5	5 - 7	> 7	3%	a) Maintaining the financial and other advantages offered by COMOTI for employees.

For the first period Balanced Scorecard is on yellow, then all the periods are on green table 2 illustrates.

Table 2. Balanced Scorecard results on 34SOL/2021 contract

1 October-31 December 2021	1 January-30 June 2022	1 July-31 December 2022	1 January-30 June 2023 (estimated)
S	1,25xS	1,30xS	1,53xS

According to the measurements established and shown in table 1, there was calculated the value of Balanced Scorecard for each period. The values for each measurement calculated for each period are considered confidential due to the fact that the contract is not finalised and has clear provisions in this area. That is the reason for which Balanced Scorecard values obtained for first period 1 January-30 June 2022 are notated with S. The value of S is considered both confidential and preliminary. First period is on yellow meaning the financial monitoring is nor bad, nor good. This result is caused by the very good values related to objectives such as “Create Value-Added”, “Endowment of Research Departments Involved in Gas Turbine Naval Applications” and “Increase Timeliness and Punctuality of Payments” but the measurements established under the Internal Process perspective registered poor values. This outcome is considered normal being at the beginning of the project implementation. Next Balanced Scorecards calculated show a good direction of the project and of financial management process.

5. CONCLUSION

The financial management on 34SOL/2021 is going on a good path. The errors encountered were corrected in order to apply continuous improvement in related processes. A positive path is due to experience of management staff. Communication between internal teams has improved and needs also to be developed. Assistance for partners with no experience in managing projects with financing from budget state should be offered. Level of budget allocated to partner should be proportionated with the time spent on its financial report.

The designed Balanced Scorecard for 34SOL/2021 project dedicated to financial assessment sets the foundations for strengthening the monitoring process of similar projects. It needs permanent improvements and adjustments. The future research will be dedicated to the finalisation of the methodology presented in this article. The project is not ended and therefore the final financial and technical assessment from UEFISCDI and the beneficiary are expected and the present methodology will be adapted if it is the case. The target is to create a solid methodology translated in an internal handbook that includes a list of standard objectives and measurements, the sources for collecting data and basic templates for calculating Balanced Scorecard for each research project implemented by COMOTI. Recommendations for future researchers that will develop a methodology to implement Balanced Scorecard are:

- To implement a Balanced Scorecard methodology for the projects with a big amount of money financed from state budget. For projects with less budget, a set of well-defined KPIs are considered sufficient. Balanced Scorecard is consuming time and resources.

- To assure a standardise assessment of partners involved in order to know how to prevent possible risks in the financial reporting. The assessment will be carried out having in mind the type of the partner organisation and their experience in managing project financed from budget state.
- To collect potential risks and measures taken to solve these issues internally.
- To ensure a methodology or at list some standardised templates at organisation level.

The implementation of Balanced Scorecard represents the step to pass from the traditional control management process to strategic management process.

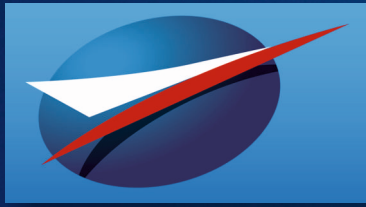
ACKNOWLEDGEMENT

This work was supported by a grant of the Ministry of Research, Innovation and Digitization, CNCS/CCCDI - UEFISCDI, project number PN-III-P2-2.1-SOL-2021-2-0169, within PNCDI III.

REFERENCES

- [1] *Strategy 2005-2008*, Hungarian Central Statistical Office, Budapest, 2005;
- [2] NUTS - common classification of territorial units for statistics; The European Union Regulation can be found on EUR-Lex Portal of European Union law: <https://eur-lex.europa.eu/legal-content/EN/TXT/?qid=1412076782293&uri=CELEX:32008R0176>;
- NUTS classification is used by policy-makers at European Union level, NUTS 1 means major socio-economic regions, NUTS 2 means basic regions for the application of regional policies; NUTS 3 means small regions for specific diagnoses (source: <https://ec.europa.eu/eurostat/web/nuts/background>)
- [3] Robert S. Kaplan, David P. Norton; *The Balanced Scorecard—Measures that Drive Performance*, Harvard Business Review, January-February 1992;
- [4] Paul R. Niven; *Balanced Scorecard Step-by-step: Maximizing Performance and Maintaining Results*; Second edition, 2006;
- [5] Udeemy; Building a Balanced Scorecard on-line training. Accessed on the 27th of January 2023; <https://www.udemy.com/course/building-balanced-scorecard/>- trainer Matt Evans.
- [6] Robert S. Kaplan, David P. Norton; *The Strategy-Focused Organisation. How Balanced Scorecard Companies Thrive in the New Business Environment*; Harvard Business School Press; 2000;
- [7] Robert S. Kaplan, David P. Norton; *The Balanced Scorecard Translating Strategy into Action*; Harvard Business School Press Boston, Massachusetts; 1996;
- [8] Planergy. *Invoice Cycle Time: What Is It and How to Improve It*; Accessed on the 15th of May 2023; <https://planergy.com/blog/invoice-cycle-time/>

Disclaimer/Publisher's Note: The statements, opinions and data contained in all publications are solely those of the individual author(s) and contributor(s) and not of COMOTI or the editor(s). COMOTI and/or the editor(s) disclaim responsibility for any injury to people or property resulting from any ideas, methods, instructions or products referred to in the content.



54th INTERNATIONAL PARIS AIR SHOW

✈️ PARIS | LE BOURGET

📅 JUNE 19-25, 2023

COMOTI - Romanian Research & Development Institute for Gas Turbines attended, with its own exhibition stand, the 54th edition of the Paris Air Show between 19-25 June 2023.



The Paris Air Show is the largest and oldest event in the world dedicated to the aviation and space industry, where the most important companies in the field meet and where the latest technologies and products are presented.

During the four days dedicated exclusively to professionals, there were visits to our stand as well as discussions with our professional partners. It is worth mentioning the invitation received and the participation at the MTU Aero Engines chalet at the preliminary

meeting to establish a consortium led by the future JV between Safran Helicopter Engines and MTU Aero Engines for the purpose of developing a helicopter engine in a technical range that does not exist in Europe (imported only).



The only specialized company that integrates
such activities as

scientific research,
design,
manufacturing,
testing,
experimental activities,
technologic transfer and
innovation

in the field of aircraft and industrial gas turbines and
high speed bladed machinery.

220D Iuliu Maniu Ave., 061206 Bucharest, ROMANIA,
P.O. 76, P.O.B. 174

Phone: (+4)021/434.01.98, (+4)021/434.02.31, (+4)021/434.02.40
Fax: (+4)021/434.02.41, e-mail: contact@comoti.ro

www.comoti.ro